ANALYSIS AND ELIMINATION OF HIGH TEMPERATURE NOTCH INDUCED MICROCRACK INITIATION IN INCONEL 718 NICKEL-BASED ALLOY

OMAR MENDOZA, Metallurgist

HYMAN FELDSTEIN, PhD

Metallurgical Science Center
Physical Science Branch
San Antonio Air Logistics Center
Kelly Air Force Base Texas

ANALYSIS AND ELIMINATION OF NOTCH INDUCED MICROCRACK INITIATION IN INCONEL 718

OMAR MENDOZA, Metallurgist

HYMAN FELDSTEIN, PhD

Metallurgical Science Section
Physical Sciences Branch
San Antonio Air Logistics Center
Kelly Air Force Base, Texas

ABSTRACT

A mechanism for eliminating high temperature notch induced microcrack initiation within Inconel 718 was formulated by correlating the dislocation theory of precipitation hardening with plane stress experimental results obtained at elevated temperatures. Elimination of notch sensitivity was found to be possible by means of innovative treatment that increased the average distance between precipitates in this alloy from 50 to 167 atomic spaces without a prohibitive reduction of yield strength. This distance modification is critical as it must be sufficient to enable dislocation line segments to pass between precipitate particles to avoid shearing them. Otherwise, this alloy will be susceptible to notch induced microcrack initiation. This analysis revealed that it is the spacing and not the size of the precipitates that determine the yield point of Inconel 718. Precipitation dispersion was accomplished by long duration solutioning and aging. Notched specimens subjected to this thermal treatment revealed no evidence of premature crack initiations. Also, heat treatment of an aircraft part that had experienced extensive in-service transformation of its strengthening gamma prime precipitates to delta phase platelets resulted in a discernible reduction of this deleterious phase without an excessive loss of tensile strength. Finally, it was found that hardness testing is inconclusive for evaluating heat treat precipitation hardening procedures and should be replaced by a static shear or tensile yield point test at the service operating temperature, combined with a determination of the average distance between precipitates to ascertain the material's notch sensitivity. This work demonstrates that the dislocation theory can be successfully applied to increasing the reliability of aerospace materials.

INTRODUCTION

1. BACKGROUND

Nickel base superalloys, although outstanding with respect to high temperature strength, are quite difficult to weld. In the 1950s, Inconel 718 was developed to fill this particular need. Inconel 718 is characterized as a weldable material because it provides a sluggish response to hardening/heat treatment rates, where weld heat affected zone hardening is minimized. The formula for providing this property consists of: (a) substitution of niobium for much of the aluminum and titanium, (b) introduction of 17% iron, and (c) reduction of the amounts of cobalt and molybdenum. However, the effect of these design alloy differences reduces the overall high temperature capability down to a maximum of 1200°F.

Since its introduction, Inconel 718 has broadened its areas of application into cryogenic and aerospace fields. Today it is considered the state-of-the-art metal and is used on many critical turbine engine components.

Despite its use by major engine manufacturers and almost 4 decades of field experience, Inconel 718 continues to be plagued with severe cracking problems that still exist today. The following cites several Air Force examples:

(1) The cause of the failures were shoulder pins manufactured from Inconel 718 which had cracked.

(2) Overhaul facilities regularly weld cracked engine components. One of the metals with the highest population requiring crack repair is Inconel 718. This alloy is also responsible for a high rework rate since additional cracks occur after the repaired parts have been through certain repair cycles, and heat treatments.

(3) Fluorescent Penetrant Inspection is used to detect surface cracks in engine components. Experience shows cracks in Inconel 718 alloy to be highly elusive to this inspection technique. The confidence level in detecting the highest possible percentages of cracks is very low. Inconel 718 cracks are virtually invisible to radiographic techniques for reasons explained furthur in this text.

(4) The augmentor liner uses Inconel 718 for reinforcement bands. These bands crack in service, contributing to the augmentor being the number one cause for engine removals.

This work analyzes the primary factors that cause the deleterious cracking of Inconel 718, and explores the possibility of reducing these causes.

2. PRELIMINARY FINDINGS.

Several Inconel 718 parts were evaluated, with primary emphasis given to the TF39 Compressor Rear Frame (CRF) which exhibits extensive cracking of the forward flange. The 1988 Actuarial Function data shows CRF cracking as the number 2 cause of worldwide engine removals (Figure 1).

3. VISUAL AND MICROSTRUCTURAL EXAMINATION.

Replicas normal to the fracture surfaces were made on CRF service induced cracked forward flanges. The replications were examined under a optical microscope and exhibited noncontinuous crack profiles indicating multiple initiation sites. This suggested that subsurface multiple origin microcracking may be occurring, with all microcracks not reaching the surface at the same time. Cross sections of the forward portion of the CRF adjacent to the flange were mounted, polished, etched and studied. The observed microstructures exhibited a relatively high density of delta phase platelets, (Figure 2), formed due to the solid state transformation. The delta phase in Inconel 718 is normally in a globular shape and it manifests itself primarily at the grain boundaries. This normal microstructure is shown in Figure 3. Globular delta phases impart certain desirable properties to the alloy such as pinning down of the grains for optimization of stress rupture ductility. However, the formation of platelets of delta degrades the alloy by depleting the hardening phase γ'. The brittle delta platelets are an incoherent, orthorhombic, nickel and niobium rich phase that precipitates at elevated temperatures in a Widmanstätten-type structure. The platelets act as stress raisers throughout the material to detrimentally affect the high temperature fracture properties of the alloy. It is this transformation that sets the temperature-time limits for engine applications.

A cross section of an Inconel 718 crack (Figure 4), showing failure of the fracture surfaces to separate, displays the characteristics of a tight line crack rather than the usual wedge shape typical of other alloys. The resulting lack of occurrence of capillary action, combined with surface disturbances and disadvantageous orientation, obscures the crack beyond the detection limits of fluorescent penetrant and radiography* techniques.

* Insufficient density difference.

A-NOTCH SENSITIVE CRACKING AND PRECIPITATE DEPLETION

A-1. INTRODUCTION.

The in-service degradation of Inconel 718 components parts is a two fold problem consisting of:

a. The mechanism responsible for premature crack initiation and

b. A solid state transformation that depletes the material of its hardening precipitates, thereby weakening the material.

c. The first of these phenomena called Notch Induced Microcrack Initiation*, is known to occur in two alloys within the Air Force inventory: Waspaloy and Inconel 718.

Notch Induced Microcrack Initiation

Notch Induced Microcrack Initiation is the susceptibility for premature crack initiation to occur at elevated temperatures, in the vicinity of a notch or stress raiser, as a function of time at a constant external stress below the yield stress as compared to an identical unnotched specimen. This is followed by subsequent crack propagation by any number of mechanisms to critical crack length and ultimate fracture. Notch Induced Microcrack Initiation is a phenomena where premature crack initiation occurs at elevated temperatures, caused by the effects of ordinary room temperature plastic deformation combined with plastic deformation due to creep.

The second of the detrimental effects is the transformation of γ'' (gamma double prime), a coherent hardening precipitate of chemical compound (Ni_3Cb). This precipitate exists in a metastable body centered tetragonal structure and is allotropically transformed into an orthorhombic noncoherent δ (delta) phase of the same chemical composition:

$$\underset{\text{Body Centered Tetragonal}}{\gamma''\ (Ni_3Cb)} \text{ ----------} \rangle \underset{\text{Orthorhombic}}{\delta\ (Ni_3Cb)} \qquad (1)$$

This transformation depletes the alloy of its strengthening properties and depending on the form taken by the resulting delta phase, it may impart stress concentration inside the grains.

A theoretical and experimental development of the elements of Notch Induced Microcrack Initiation is first presented, showing the steps required to eliminate its occurrence. This is followed by an in-depth analysis of the mechanism of the γ'' ---) δ transformation. The two phenomena are then combined and related to experimental results obtained in the heat treatment of Inconel 718. From the above results a heat treat procedure is formulated that completely eliminates Notch Induced Microcrack Initiation and considerably reduces the existence of delta platelets. (A complete description of the dispersed phase structures that control the in-service behavior and properties of Inconel 718 is presented in a subsequent addendum).

* Formerly called Time Dependent Notch Sensitivity

NOTCH INDUCED MICROCRACK INITIATION

A-2. PHYSICAL FRACTURE CHARACTERISTICS OF NOTCH INDUCED MICROCRACK INITIATION

Consider a failed notched tensile specimen* tested under a constant load below the yield point at a temperature between 1000°F and 1400°F. Examination of the fracture shows it to consist of two distinct portions. The initial part or slow growth portion began at the notch and extended intergranularly in a direction perpendicular to the loading direction and was discolored from oxidation. (Figures 5 and 6). The remainder or fast fracture portion (not shown), was a transgranular 'through thickness' shear failure that was not discolored by oxidation.(1)

Critical to the crack initiation was localized plastic yielding at the base of the notch upon loading, followed by subsequent creep deformation at the grain boundaries(1). Both phenomena contributed to crack initiation, as they alleviated the stress concentrations introduced by the existence of a notch.(1) Slow crack extension then occurred primarily by plastic deformation, as evidenced by a coalescence of voids or dimpled region on the fracture surface, as the crack tip advanced across the specimen(1). Ultimate transgranular fracture occurred when the critical crack length corresponding to the external load was reached.

The notch sensitive cracks initiated after 60% of the rupture life as compared to 95% - 97% in the unnotched specimen, where the intergranular cracks initiated randomly within the gauge length(1).

B. THEORETICAL DEVELOPMENT.

B-1. DEVELOPMENT OF BASIC FUNDAMENTALS.

In order to develop the concept of crack initiation due to Notch Induced Microcrack Initiation, it is necessary to interpret its mechanism in terms of an analysis of precipitation hardening of coherent dispersed particles. The theory is attributed to Mott, Nebarro, Cottrell and Orowan(4).

'A dispersed phase is said to be coherent with the matrix lattice when there is no discreet interface existent between the two phases. This necessitates that the lattice periodicity and spacing of the dispersed phase closely match those of the matrix phase across their common planar surface. Any deviation in this lattice match is accommodated by either local elastic strains in both crystal lattices, or by the presence of a defect, or by a combination of both elastic strains and defect structure. (The defect is usually a dislocation structure within the planar interface)'(3).

* The specimens were heat treated with a notch sensitive procedure, in accordance with the heat treats of current industrial applications. A complete theory of precipitation hardening must cover the range of values the flow stress takes from the solution treated condition before the saturated solid solution has decomposed, (zero size precipitates) up until the overaged condition where the precipitates are so large that they fail to adequately act as a strengthening mechanism.

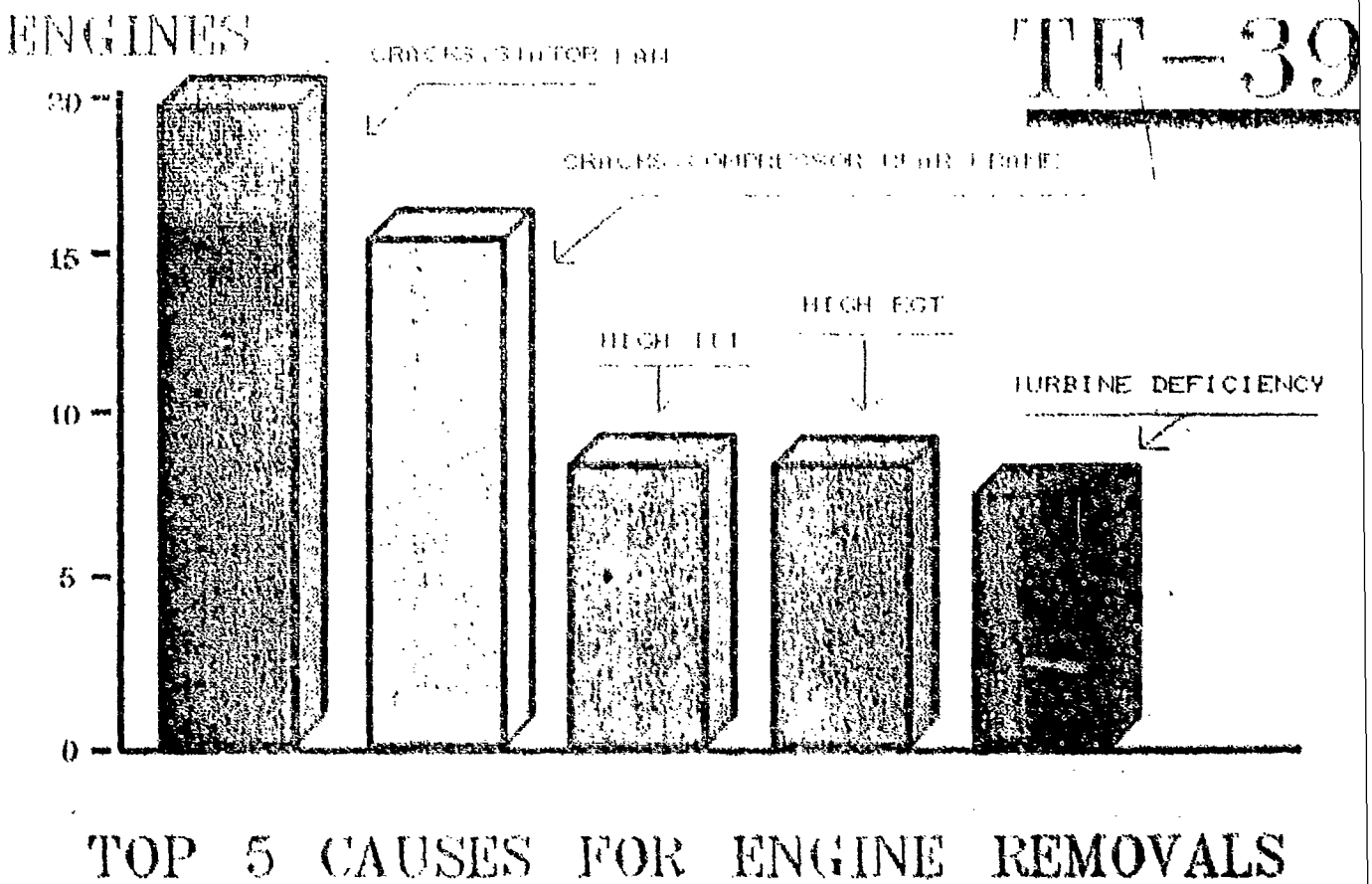

TOP 5 CAUSES FOR ENGINE REMOVALS

Figure 1 - Materiel Management actuarial function data for 1988, showing the five major causes for engine removal.

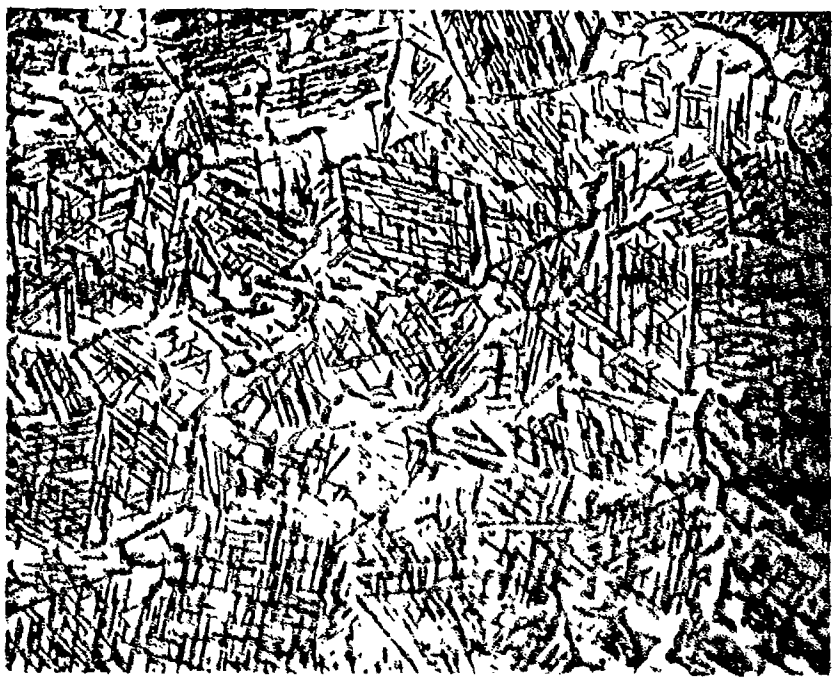

Figure 2 - (1000x) (Marbles etch)

Optical micrograph of microstructure of Inconel 718, taken from a Compressor Rear Frame removed from service. The needles are the projection of the platelets of delta phase in a Widmanstätten structure, according to the reaction:

γ' (Ni_3Cb) ----------) δ (Ni_3Cb)
Body Centered Tetragonal Orthorhombic

Heat treat procedure: Solution Treat -------) 1,700°F for 1 hour
Age ----------) 1,300°F for 8 hours
1,150°F for 8 hours

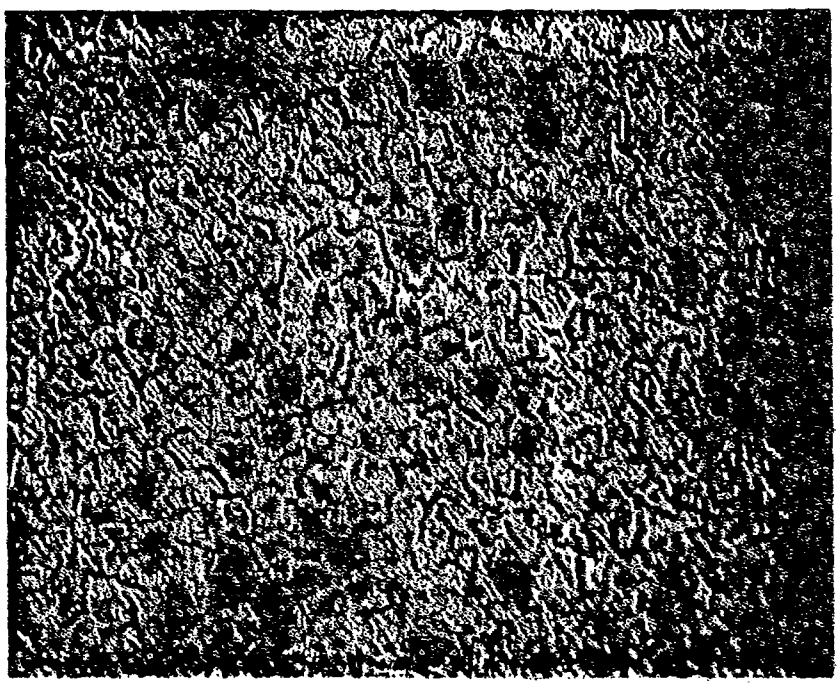

Figure 3 - (1000x) (Marbles etch)

Optical micrograph of microstructure of Inconel 718 virgin material, taken from a Compressor Rear Frame flange, that did not see service. Note the undeformed grains with globular delta phase at the grain boundaries.

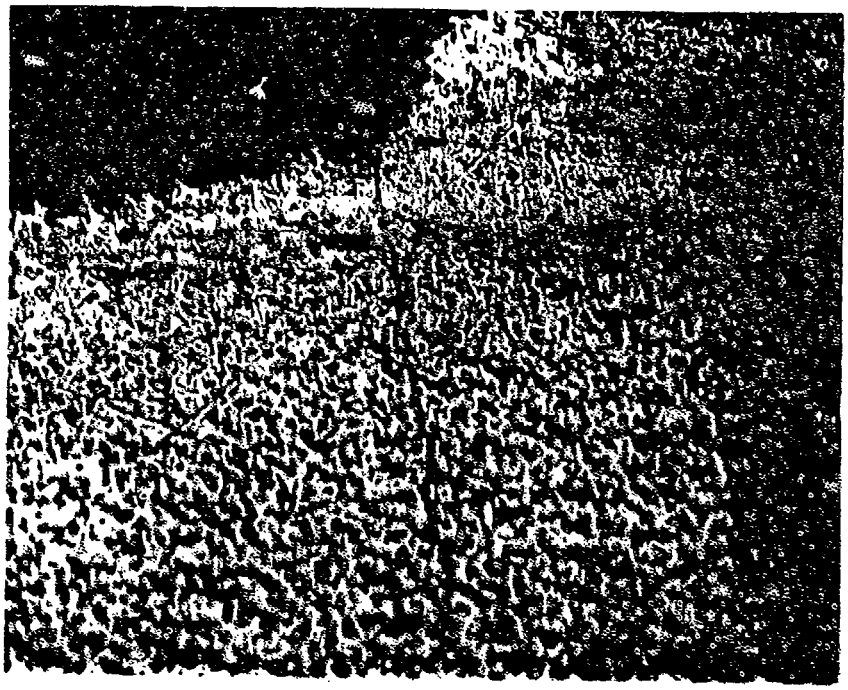

Figure 4 - (1000x) (Marbles etch)

Optical micrograph of a notch induced line crack profile in a failed Inconel 718 augmentor liner shoulder pin.

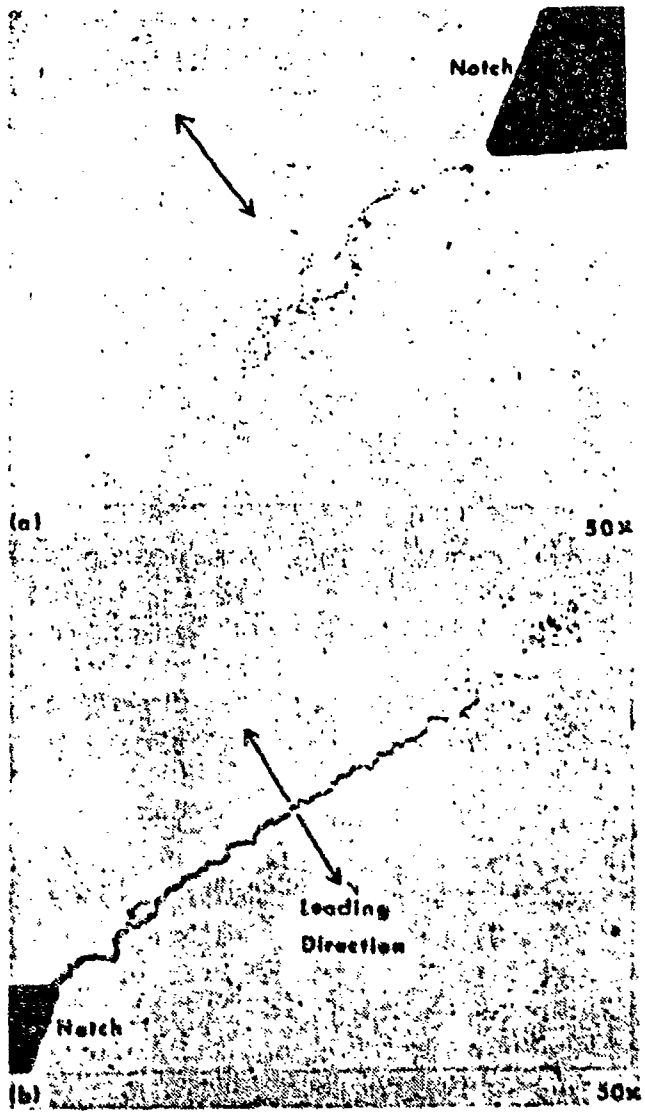

Figure 5 - (50x)

(Polished but not etched) Optical micrograph of a double notched specimen of Waspaloy, heat treated with a notch sensitive procedure, tested at 1000°F at 80 ksi for 90% of its rupture life.

a. Microcracks are in an early stage of crack initiation.

b. 'Through thickness' crack at a later stage of intergranular crack growth (Reference 1).

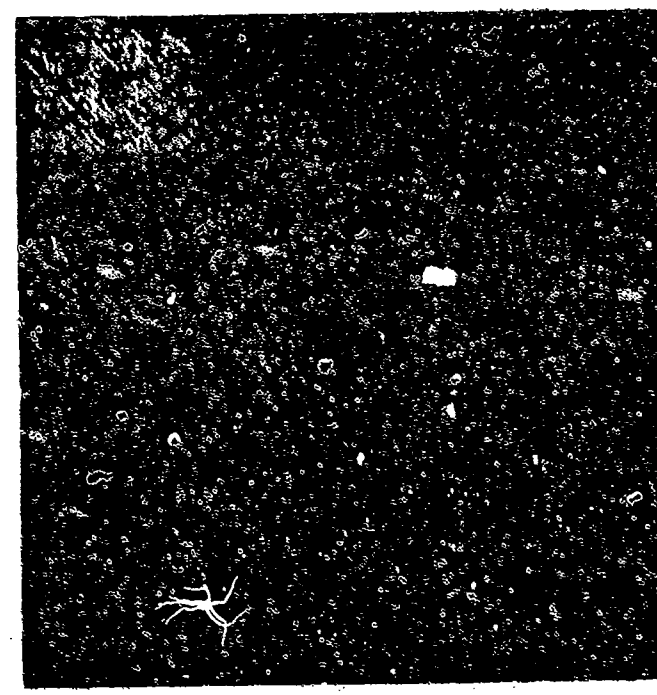

Figure 6 - (500x)

(Polished but not etched) Optical micrograph of a notch induced intergranular microcrack, in the early stages of crack development. The part is a Pratt and Whitney engine component, manufactured from Inconel 718 and heat treated with a notch sensitive procedure. (Service condition 1000°F-1200°F).

The flow stress* is the value of the critically resolved shear stress that is necessary to(s):

(1) Move the immobilized dislocations to free them from their precipitate barriers.

(2) Move these freed dislocations to overcome the Peierls stress so that they glide in their slip system and move out of the material, and

(3) Activate new dislocation sources and therefore increase the dislocation density(s).

During solidification of a polycrystalline alloy, all of the grains nucleate and grow in different directions, so that when they meet at the grain boundaries, each grain is mismatched from its neighbors. Slip or yielding initiates when the flow stress is reached first on one and then on a number of differently oriented slip systems within an individual grain. Slip is transmitted to adjacent grains when dislocation pileups occur at the grain boundaries, creating a stress concentration that unlocks existing dislocations from their barriers and activates new dislocation sources in the neighboring grains. When a dislocation has expanded to the boundary of the specimen, it moves out of the material, and the dislocation is annihilated, reducing the energy of the system. The top part of the metal has been displaced by one atomic distance with respect to the bottom part, and the material is said to have yielded. It is the immediate release of this annihilation energy by a multitude of dislocations that simultaneously surmount their barriers, in an avalanche of dislocation breakaway, with subsequent movement out of the material, that is responsible for the yield point.

To strengthen a material, the increase in yield stress depends largely on the strength, structure, spacing, size, shape, and distribution of the precipitate particles as well as on their degree of misfit. When an isolated solute atom is present in the solution treated condition, it creates a degree of misfit ε in the solvent crystal, so that the atomic radii of the solvent and solute atoms are given by r_o and $r_o(1+\varepsilon)$ respectively. Any size coherent spherical particle that encloses a given group of lattice sites, changes its radius by the factor $(1+\varepsilon)$ so that the degree of misfit of a spherical particle is independent of its size. The precipitate particles are dispersed in the alloy material to create a strain field that produces residual microstresses that act as barriers to dislocation motion and gives the material its yield strength. The shear strain associated with these microstresses at a distance R from a spherical inclusion of radius r_o and misfit ε is given by the theory of elasticity to be:

$$\text{Strain} = \frac{\varepsilon r_o^3}{R^3} \qquad (R > r_o) \qquad (1)$$

* The flow stress or critical resolved shear stress is the yield point in shear.

When a supersaturated solid solution is freshly quenched from the solution treated condition the particles consist of many solute atoms dispersed within the material matrix an average distance Ω of about 3 atomic spaces apart(4). When this material is raised to the aging temperature, the formation of a second phase occurs by nucleation and growth of the precipitate particles as a result of diffusion of the solute atoms. As the distance Ω, between precipitate particles increases, many small particles are replaced by fewer large ones, and the hardness and yield strength increase to a maximum, for the fully aged alloy. When this happens the immobilized dislocation line segments must surmount a potential barrier(3, 4) that is characterized by a critical dispersion size or critical average distance between precipitates Ω_c. If the aging treatment was allowed to continue, the alloy becomes soft again, and is said to be averaged. This is when the dispersion size exceeds the critical distance, and then continues to increase with increased hours of aging. Since ε is constant, regardless of precipitate size, softening occurs when changes in the state of dispersion take place, without changes in ε.

It is shown in the next section, that it is this critical distance Ω_c, that must be exceeded for a dislocation line segment to pass between two precipitate particles without shearing them. Then the critical spacing Ω_c determines the maximum yield point and not the size of precipitate. It is this mechanism that must act, when yielding is incipient at the base of a notch to completely eliminate Notch Induced Microcrack Initiation.

Lets assume that the yield point stress of an alloy is due to the average arithmetic mean of the internal stress that acts at a distance from a given dislocation line segment, due to coherent spherical precipitate particles dispersed throughout the material matrix. Mott and Nebarro(4) derived* an expression for this average internal shear stress or yield point stress that immobilizes a dislocation:

$$\sigma_i = 2\,G\,\varepsilon\,C \qquad (2)$$

Where:

G = Shear modulus of elasticity $\frac{lbs}{in^2}$

ε = Degree of misfit $\frac{r_o - r_i}{r_i}$ $\frac{in}{in}$

r_o = Radius of solute in

r_i = Radius of solvent in

C = Volume fraction of precipitate volume/volume

* Let the average distance from any point in the matrix to the nearest precipitate particle be $1/2(N)^{1/3}$ in a material containing N particles per unit volume, each of radius r_o and misfit ε. Substituting in eq(1) gives a strain of approximately $8\varepsilon r_o^3 N$, and when the concentration of solute $C \simeq (4/3)\pi r_o^3 N$, is inserted, equation (2) is obtained.

Note that this result for σ_i, the flow stress, is independent of: (a) Ω, the distance between precipitates, (b) the crystallographic structure of the alloy and (c) the dislocation density, but depends very strongly on: (a) the shear modulus of the matrix material, (b) the degree of misfit of the precipitate in the host material and (c) the volume fraction of the precipitate when the alloy is at its maximum yield point.

If one now considers a rigid straight dislocation line segment, equation (2) suggests that the solute atoms should fully harden the alloy, regardless of dispersion size, since it is independent of Ω. Alternatively, one can say that a straight dislocation line is acted on by randomly alternating stress fields, some of which push the individual dislocation segments forward and others that push other segments backward, so that the algebraic average of all stresses cancel one another and there is no hardening. Mott and Nebarro(4) then postulated that the theory was incomplete, since the dislocation line was not rigid, and individually pinned segments have the flexibility to move independently of neighboring segments to bend around regions of high interaction energy so the random forces do not all cancel. This would explain the effect of the scale of dispersion. Hence, the extent to which one section of the line can move independently of its neighbors, depends on the distance between them, Ω.

Cottrell(4) then related the limiting radius of curvature R, to which a pinned dislocation line segment can be bent to the flow stress σ_i, by the principle that a curved dislocation line can be held in equilibrium in the shape of a curve, only when it is acted on by an outward shear force due to an applied external stress(4, 5). The shear force acts normal to the dislocation line segment and is balanced in equilibrium, by an opposing inward force component due to the line tension at the ends of the segment. Balancing these two forces, he arrived at the following result(4, 5):

$$R = \frac{\alpha G b}{\sigma_i} \qquad (3)^*$$

with α having the value of .5.

G = Shear modulus of elasticity

b = Burgers Vector

σ_i = Flow stress

Cottrell(4) then compared R with Ω, and showed that the maximum radius of curvature that a dislocation line segment can be bent corresponds to the maximum yield stress of the fully aged alloy when R is of the order of magnitude of Ω_c:

$$\Omega_c \simeq R = \frac{.5 G b}{\sigma_i} \qquad (4)$$

When $\Omega = \Omega_c$, the dislocation can bend the maximum amount possible round regions of high interaction energy, and when slip occurs, the line segment overcomes the maximum potential energy barrier from one energy valley to the next.

* Equation 3 is derived in Ref (4).

Since σ_i is independent of Ω in equation(2), Cottrell substituted(2) into (4) and used his values of $\varepsilon = 1/5$ and $C = 1/40$ to establish his criteria for the critical dispersion size(4).

$$\Omega_c \simeq R = \frac{.5\ G\ b}{\sigma_i} = \frac{.5b}{2\varepsilon C} = \frac{.5b}{(2)(1/5)(1/40)} = 50b \qquad (5)$$

For the alloy to be in the fully aged condition, the average distance between precipitates is in the order of 50 atomic distances. When $\Omega < \Omega_c$ the material is underaged and softened. When $\Omega > \Omega_c$, the material is overaged and is softened, as the yield point decreases with increased aging time, (Figure 7). This suggests that the precipitate size increases as the distance between precipitates exceeds the limiting radius of curvature, for the critical dispersion size given in equation (4) by Mott, Nebarro and Cottrell(4).

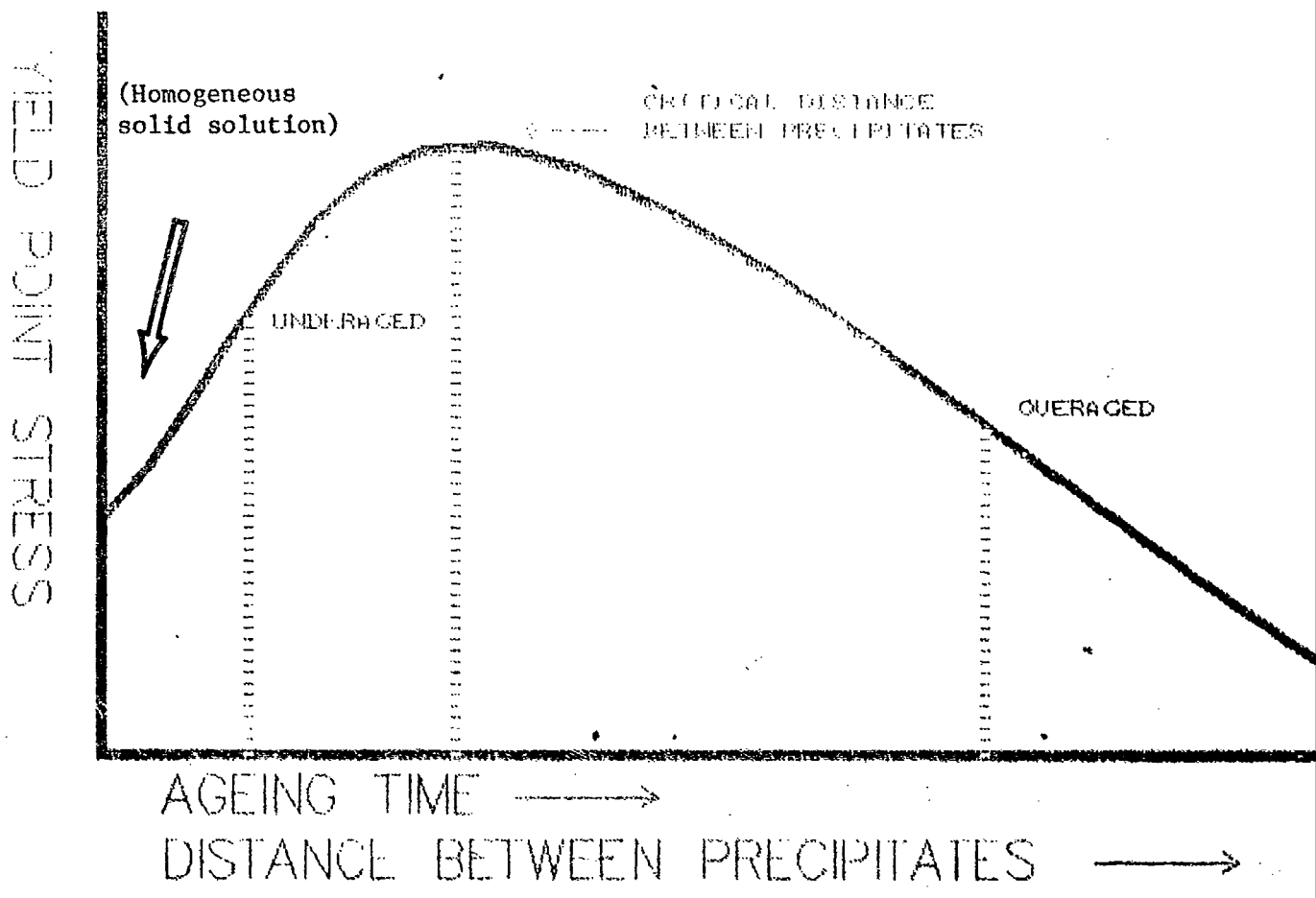

Figure 7 - Schematic representation of the shear yield point as a function of aging time or atomic distance between precipitates, showing the underaged, critically aged and overaged heat treatments.

Orowan[4] later proposed that, in an overaged alloy, the dislocation line segments are pinned by widely spaced obstacles and do not have to overcome a large potential barrier to initiate the flow stress, but bulge instead into the spaces between obstacles (Figure 8). As this occurs, the applied stress increases until adjacent sides of neighboring loops join together to bypass the obstacles, so that the line segments pass between them. The precipitates are left encircled by small ring segments of the released dislocation, which act as additional obstacles that increase the flow stress on subsequent dislocations. The flow stress required for yield to occur is the shear stress that will bend the dislocation line segment into loops of $\Omega/2$. By equating the limiting of radius of curvature $\frac{\alpha G b}{\sigma_i}$ to $\Omega/2$, Orowan arrived at:

$$\sigma_i = \frac{2 \alpha G b}{\Omega} \qquad (6)$$

Where $\alpha = .5$.

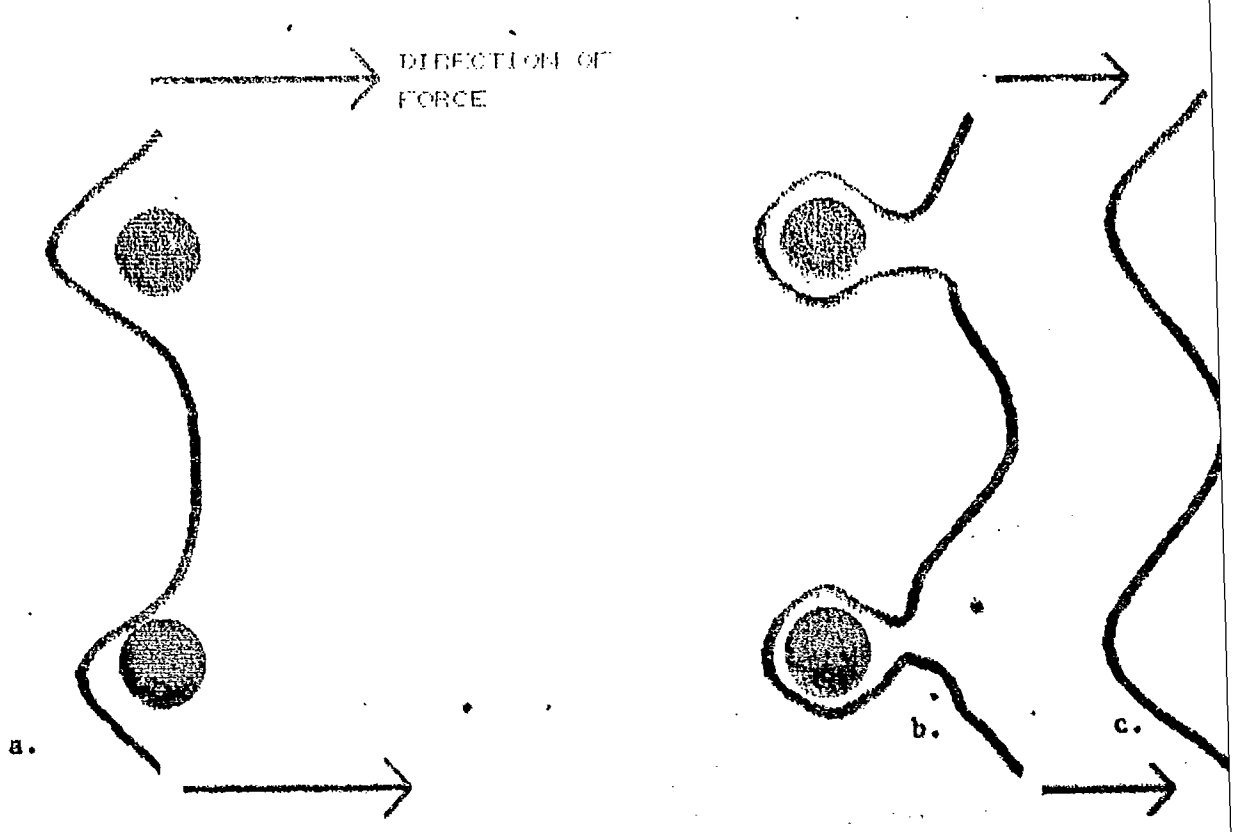

Figure 8 - Dislocation mechanism for overaged alloy. Dislocation passes between precipitates when the distance between particles exceeds the limiting radius of curvature to which the dislocation can be bent.

a. Applied stress overcomes internal stress. Dislocation bulges into region between the obstacles.

b. The bulging increases as the external stress increases until eventually adjacent sides of neighboring loops join together.

c. The dislocation passes between the obstacles, leaving them enclosed by small ring segments of the released dislocation.

Hence, the flow stress decreases inversely with the scale of dispersion for the overaged alloy. As precipitate growth takes place, Orowans above process replaces that of Mott, Nebarro and Cottrell[4] and the dislocations pass between the precipitates, almost as soon as the scale of dispersion exceeds the critical value[4, 6, 7]. This precludes the premature shearing of precipitates by the dislocations.

Consider now the early stages of aging from the complete solution treated condition, up to the fully aged alloy. Here, the Orowan condition does not hold, since the line segment must reach the maximum radius of curvature and first satisfy equation(5) before it can pass between particles according to equation 6. Suppose instead that the dislocation moves from A to B without appreciably departing from a straight line (Figure 9). Let γ be the energy per unit area of the interface produced when the particle is sheared, and πr^2 be the area of a precipitate of radius r. Then the energy to cut the particle is given by $\gamma(\pi r^2)$.

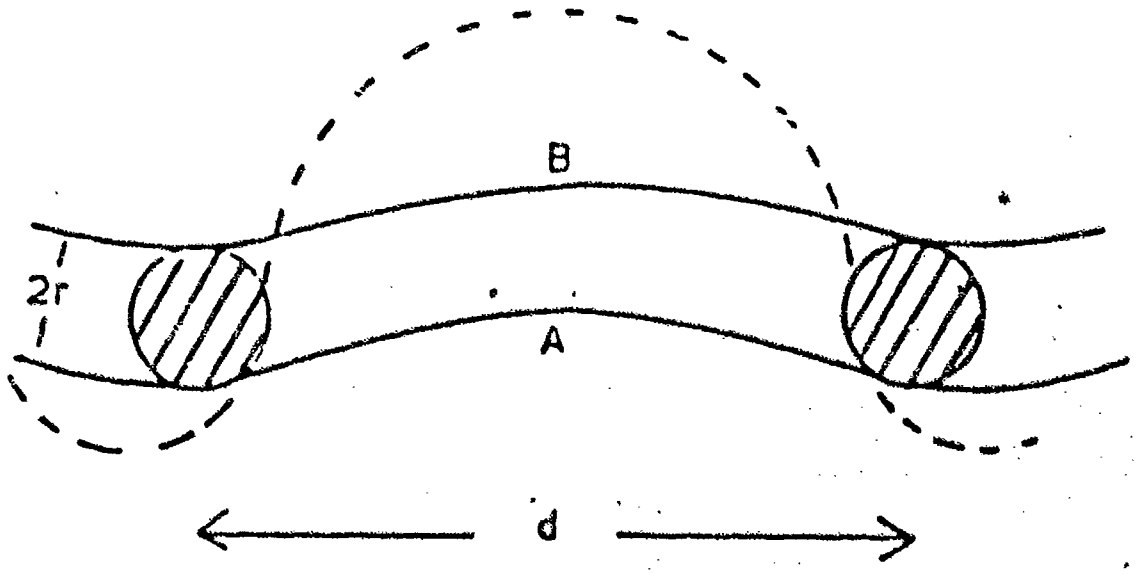

Figure 9 - A dislocation can either cut through precipitates from Position A to Position B (solid line), or else pass between them to satisfy Orowan's criteria (dotted line).

Let b be the Burgers vector of the dislocation line segment of length Ω between precipitates, and the shear force per unit length acting along the dislocation line $\sigma_{ic}b$. Equating the energy required to the work done by a dislocation as it moves from A to B:

$$\sigma_{ic}b\ \Omega\ 2r = \pi\ r^2\gamma \tag{7}$$

$$\sigma_{ic} = \frac{\pi\ \gamma r}{2\ \Omega b} \tag{8}$$

where σ_{ic} is the flow stress necessary to shear the particle. For a coherent particle:

$$\text{if } \sigma_{ic} > \sigma_i \tag{9}$$

the dislocation will circumvent the precipitate. If:

$$\sigma_{ic} < \sigma_i \tag{10}$$

the particle will be sheared.

B-2 APPLICATION TO INCONEL 718 ALLOY

Taking an actual case of Inconel 718 alloy tested at 1000°F, the manufacturer specified[8] the fully aged condition as having a tensile yield point of 135 ksi and a shear modulus, G = 9.7(10)^6 psi. Experimental results[8] related the shear yield strength to coherent γ' and γ' precipitate particles 60A in diameter, after solution treating for 1 hour at 1700°F followed by aging for 3 hours at 1325°F.

Predicting the flow stress theoretically, with the equation of Mott and Nebarro, (Equation 2) using the values of $\varepsilon = 1/5$ and $C = 1/40$ given by Cottrell[4]:

$$\sigma_i = 2\,G\,\varepsilon\,C = 2(9.7)10^6\ \text{lb/in}^2\ (1/5)(1/40) = 97{,}000\ \text{psi} \qquad (2)$$

This is the yield point stress for the fully aged alloy that immobilizes the dislocations, and that must be overcome if they are to circumvent their barriers. Substituting σ_i = 97,000 psi and G = 9.7(10)^6 psi (measured by Inco Int[8]) into Cottrell's equation gives the critical distance between precipitates:

$$\Omega = \Omega_c \simeq R = \frac{.5\,G\,b}{\sigma_i} \qquad (4)$$

$$\Omega_c = \frac{4.5)(9.7)10^6 b}{(97{,}000)} = 50b$$

This is in exact agreement with Cottrells prediction, presented earlier in equation (6) for the critical dispersion size Ω_c. The experimental results, measured the flow stress to be 67,500 psi. This was far below the value predicted here from Mott and Nebarros theory. This long range resisting force of 97,000 psi immobilized the dislocation, but since the precipitates were sheared at a lower stress:

$$\sigma_{i_c} < \sigma_i \qquad (10)$$

The dislocation passed them by the cutting process. This is confirmed by transmission electron microscopy micrographs, taken after the specimen was creep rupture tested below a yield stress of 130 ksi, which showed that the deformation was localized in slip bands (Figure 10). This microstructure showed severe Notch Induced Microcrack Initiation, with ultimate fracture occurring after 17.5 hours in the notched specimen as compared to 5813.4 hours for the unnotched specimen.

Figure 10. Transmission electron micrograph of an Inconel 718 specimen solution treated 1 hour at 1700°F followed by aging 3 hours at 1325°F and tested at 1000°F at a constant applied stress of 130 ksi (Yield Point = 135 ksi). Note the localized slip bands on the surface, signifying that the dislocations sheared the γ'/γ''* particles on the (111) slip planes, and were in pairs, separated by stacking faults. (Reference 9)

* γ'/γ'' will denote γ' and/or γ''. The characteristic X-ray spectra is very close for γ' and γ'' and therefore the difference is sometimes difficult to distinguish(9).

To find the energy necessary for the dislocation to shear the atomic bonds of the precipitate, when the flow stress, σ_{ic} = 67,500 psi, is reached, equation (8) is solved for τ with:

$$\Omega = 50b; \quad r = 30 \text{ Å}$$

b = Burgers Vector for γ matrix$_{(10)}$ = 3.59 Å

then: $$\tau = \frac{\sigma_{ic}\, 2\, \Omega\, b}{\pi\, r} = \qquad (8)$$

$$\frac{(67{,}500)\ \text{psi} \times (.06895)\ \frac{\text{dynes}}{\text{psi}} \times (2.0)(50)(3.59(10)^{-8})^2\ \text{cm}^2}{(3.1416)\ (30)10^{-8}\ \text{cm}}$$

$$\tau = 636.5\ \frac{\text{ergs}}{\text{cm}^2}$$

This is the energy required to cut through a γ' particle of Ni_3Cb in the body centered tetragonal structure. This value is a reasonable result when compared to values exceeding 1000 ergs/cm² for intermetallic compounds incoherent with the matrix of aluminum or copper alloys, and 100 ergs/cm² for Guiner-Preston zones, coherent with aluminum base alloys (8).

The above analysis has shown that the limiting factor that determines the maximum yield strength of an alloy is the length of dislocation line that can be bent to the maximum radius of curvature by the applied shear stress, and not the size of precipitate. The subject of precipitate size will be discussed in Section D. The size of precipitate is, however, very important when it is sheared by the dislocation before the maximum radius of curvature is reached. Experimental evidence will be presented shortly to show that it is this cracking of precipitates combined at identical locations with subsequent high temperature grain boundary movement that is the Notch Induced Microcrack Initiation Mechanism.

C. THE PROPOSED HEAT TREATMENT

In order to prevent Notch Induced Microcrack initiation from occurring in Inconel 718, the average atomic distance between precipitates must be increased to exceed the critical distance set forth by the theories of Mott, Nebarro and Cottrell(4). Then the dislocation line segments will bulge between obstacles, at a reduced flow stress, without shearing the particles. Of the different heat treat procedures formulated, all met the above requirements of Orowans criteria (Equation 6), and all of them were free from Notch Induced Microcrack Initiation, when tested in plane stress at 1000°F and 1200°F(8). However, only one heat treatment* met the requirements formulated in AMS 5596 for yield and ultimate stress in plane stress deformation. Analyzing this heat treat, the results showed a flow stress of σ_i = 58 ksi measured at 1000°F(8) (TEM measurements showed a particle diameter of 200Å)(8). (G = 9.7 10^6 psi at 1000°F)(6).

Inserting this result into Orowan's relation for an overaged alloy (Equation 6), gives the average dispersion size at 1000°F.

$$\Omega = \frac{2\,\alpha\,G\,b}{\sigma_i} = \frac{9.7(10)^6}{(58)\ 10^3}\,b = 167b$$

Thus, by applying this heat treat, the distance between precipitates has been increased from 50 to 167 atomic distances.

* Solution treat 10 hours at 1700°F ±25°F, furnace cool with argon; age 48 hours at 1350°F ±15°F, furnace cool.

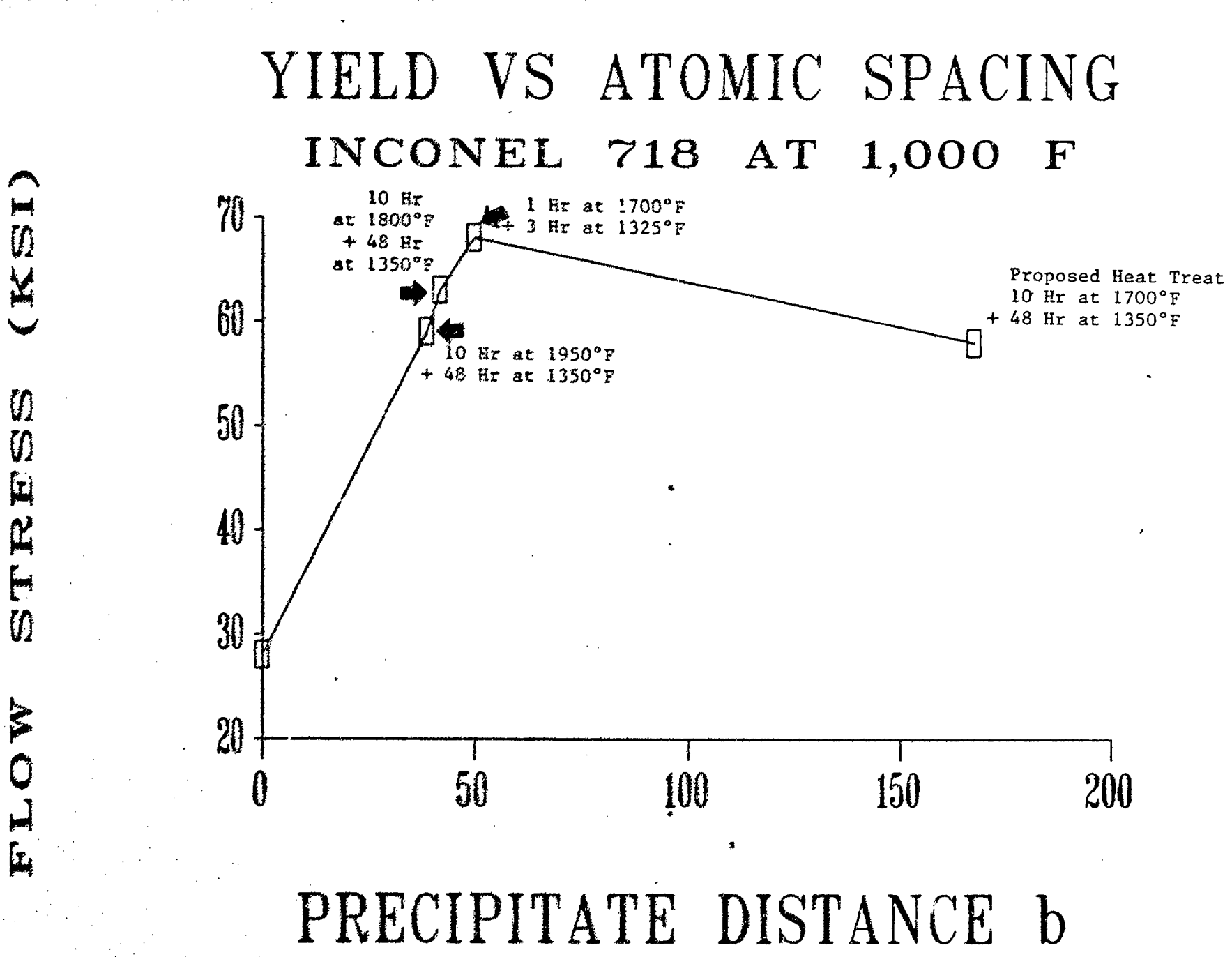

Figure 11 - Yield point as a function of atomic distance between precipitates ~~of aging time at~~ at test temp 1000°F.

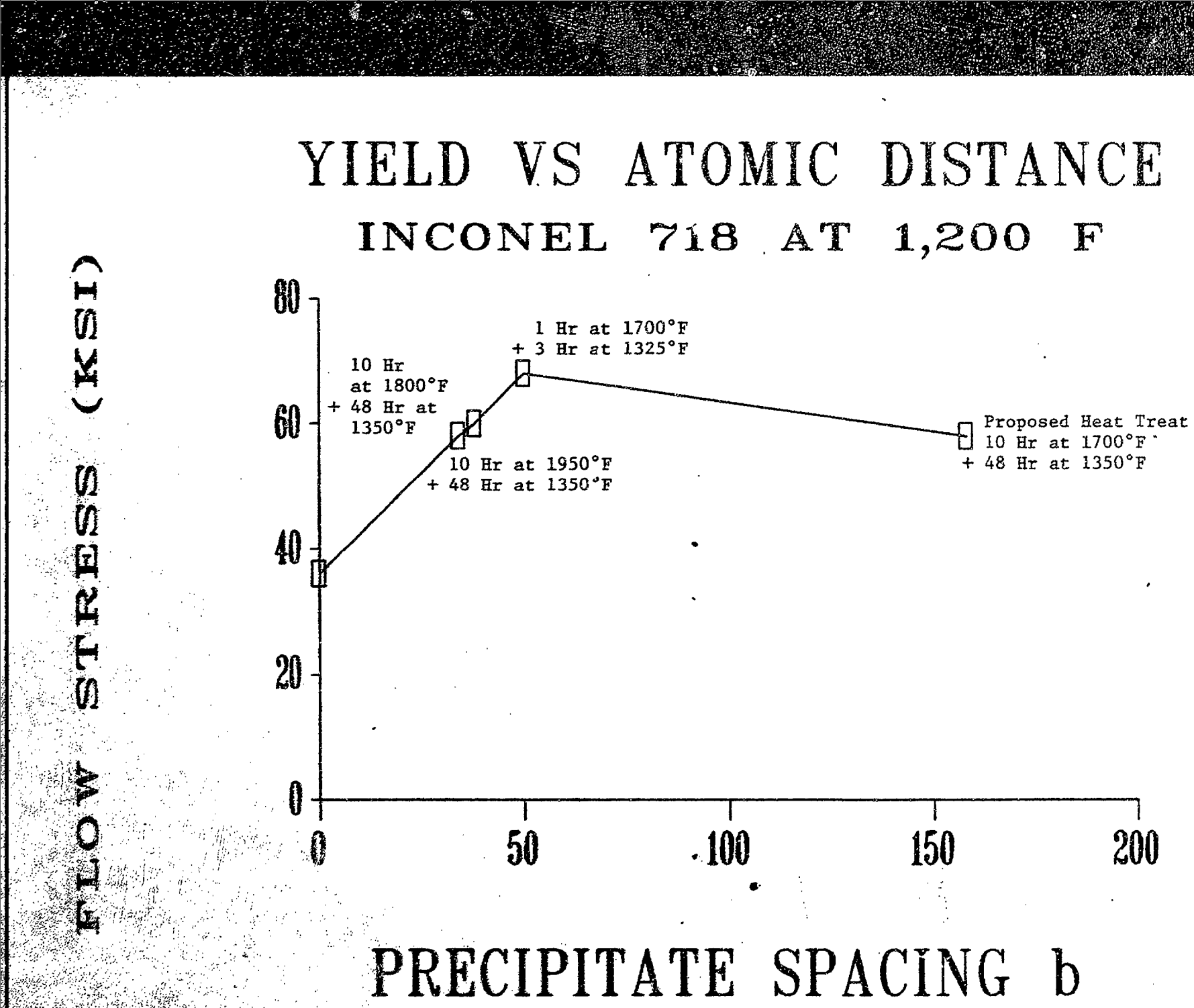

Figure 12 - Yield point as a function of atomic distance between precipitates or aging time at 1200°F.

a

b

Figure 13.

Figure 13a - TEM micrographs of Inconel 718 heat treated 1 hr at 1950°F + 48 hr at 1350°F and tested at 120 ksi, 1100°F. Slip bands appear on external surface. Dislocation moved exclusively by slip on 111 planes as they sheared the γ'/γ'' particles, to produce localized deformation. (Reference 9)

Figure 13b - TEM micrograph of identically prepared specimen as in Fig 13a, but tested at 30 ksi, 1400°F. Particle growth plus thermal fluctuations resulted in particle bypass with no localized deformation. Deformation was homogeneous, as dislocations passed between particles, bending loops around γ' particles and entanglement with γ'' particles. (Reference 9).

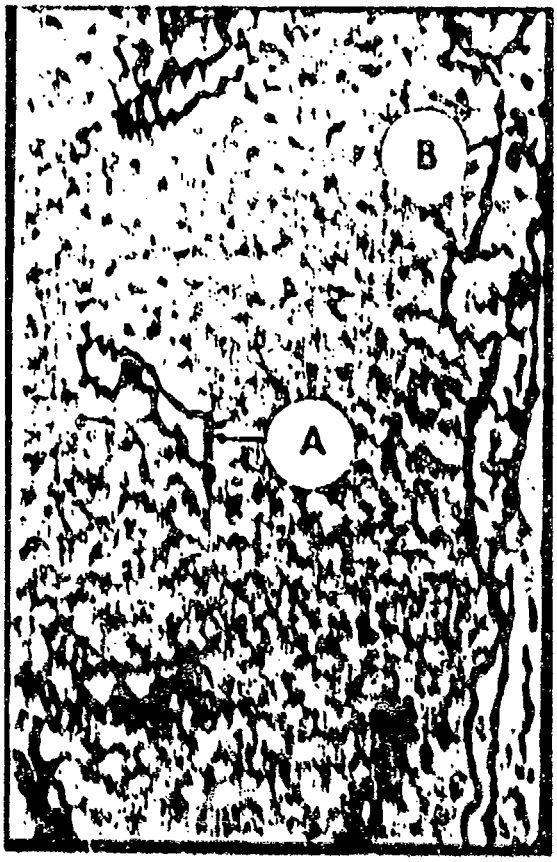

(a) Aged 455 hrs. at 1290°F (700°C). Dislocation (Orowan) loops are indicate at A and B.

(b) Aged 200 hrs. at 1380°F (750°C). At A, a loop encircles two particles.

(a) Aged 455 hrs at 1290°F (700°C). Dislocation (Orowan) loops are indicated at A and B.

(b) Aged 200 hrs at 1380°F (750°C). At A, a loop encircles two particles.

Figure 14.

Figure 14a - Paired dislocations shearing precipitate particles at critical separation distance and peak yield point. (Reference 15).

Figure 14b - Dislocation loops around precipitates in an overaged alloy. Dislocation segments greater than the critical length passed between precipitates, satisfying Orowan's criteria.

When the above flow stress, σ_i = 58 ksi required to overcome the yield stress of the material, is compared to the shear stress σ_{ic} necessary to cut through an Ni_3Cb precipitate particle, with:

$$\tau = 636.5 \text{ ergs/cm}^2 \; ; \; \Omega = 167b$$
$$r = 100\text{Å}; \; b \text{ for } \tau \text{ matrix} = 3.59\text{Å} \quad \text{(Ref 10)}$$

$$\sigma_{ic} = \frac{\pi}{2} \frac{\tau r}{\Omega b} = 134 \text{ ksi} \qquad (8)$$

The results satisfy inequality (9):

$$\sigma_{ic} > \sigma_i \quad \text{i.e.} \quad 134 \text{ ksi} > 58 \text{ ksi}$$

so that the dislocation will pass between the precipitates without shearing through them, and Notch Induced Microcrack Initiation does not occur. (Figures 8, 11, 12).

This is confirmed by the TEM micrographs that show that the dislocations were not localized in slip bands as in figures 10 and 13a, nor observed cutting through the particles as in figure 14a, but were observed entangled with and leaving loops around γ'' and γ' precipitates, after passing between them on the slip plane (Figures 13b, 14b).

Comparing the rupture lives of notched specimens of the proposed heat treatment, with notched specimens of a heat treatment that exhibited the optimum tensile yield point as given by the manufacturers specifications* shows a substantial increase in service life till fracture when Notch Induced Microcrack Initiation is eliminated (Figure 15).

* 135 ksi at 1,000°F as specified by the manufacturer, Huntington Alloy Division of International Nickel Co. in their specifications for Inconel 718 (Reference 8, P.11 Table 24).

1,000 F LIFE AT 75 KSI
NOTCHED INCONEL 718

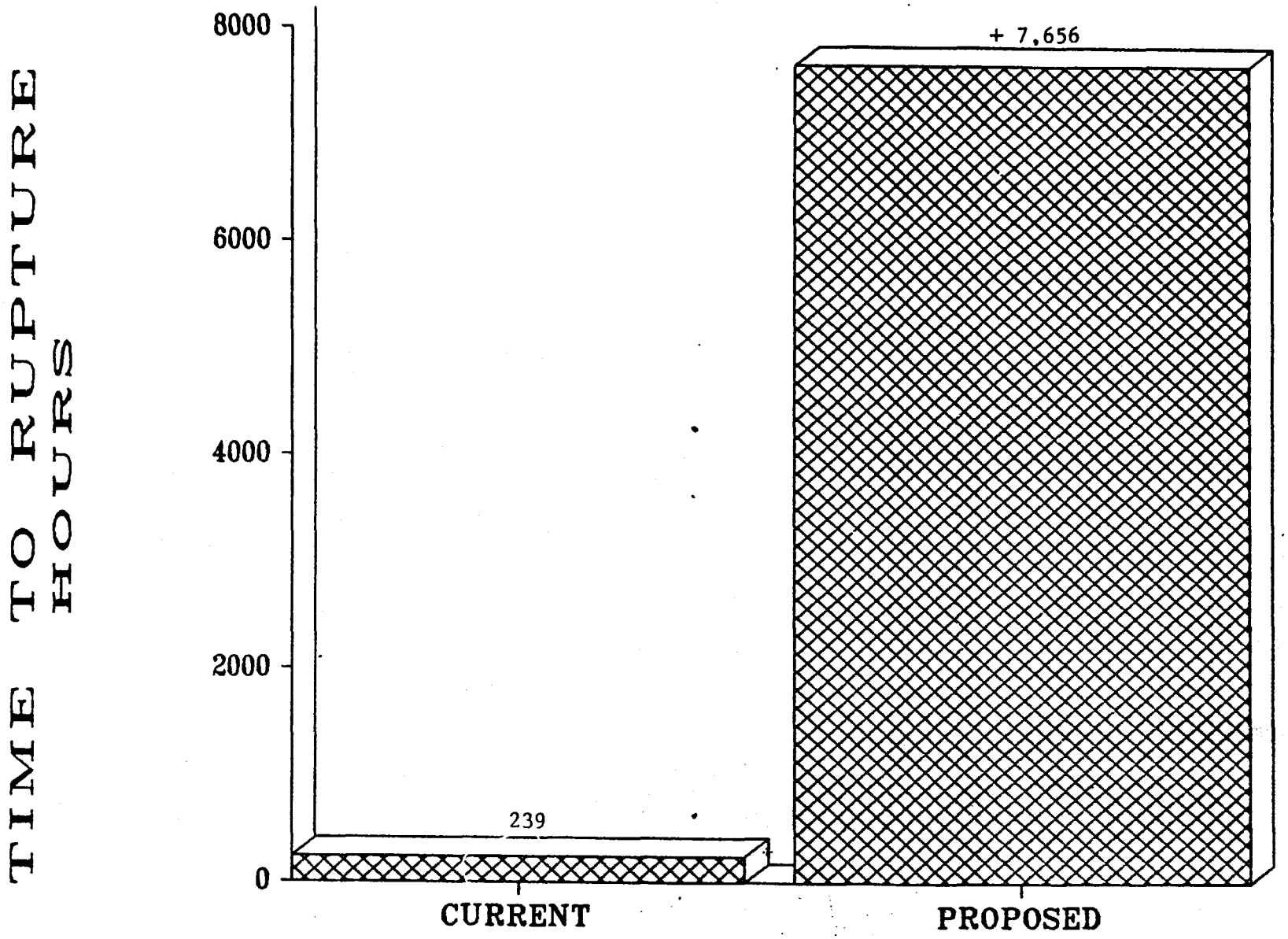

Figure 15:

Comparison of creep notch rupture life of proposed heat treatment of Inconel 718 with notch rupture life of a heat treat procedure that exhibited the optimum tensile yield point at 1000°F as specified by the manufacturer. Note that the specimen of the proposed treatment tested at 75 ksi was stopped after 7656 hours of test without fracture, as compared to the fracture of the optimum yield point specimen of 239 hours.

1,000 F RUPTURE LIFE
NOTCHED INCONEL 718

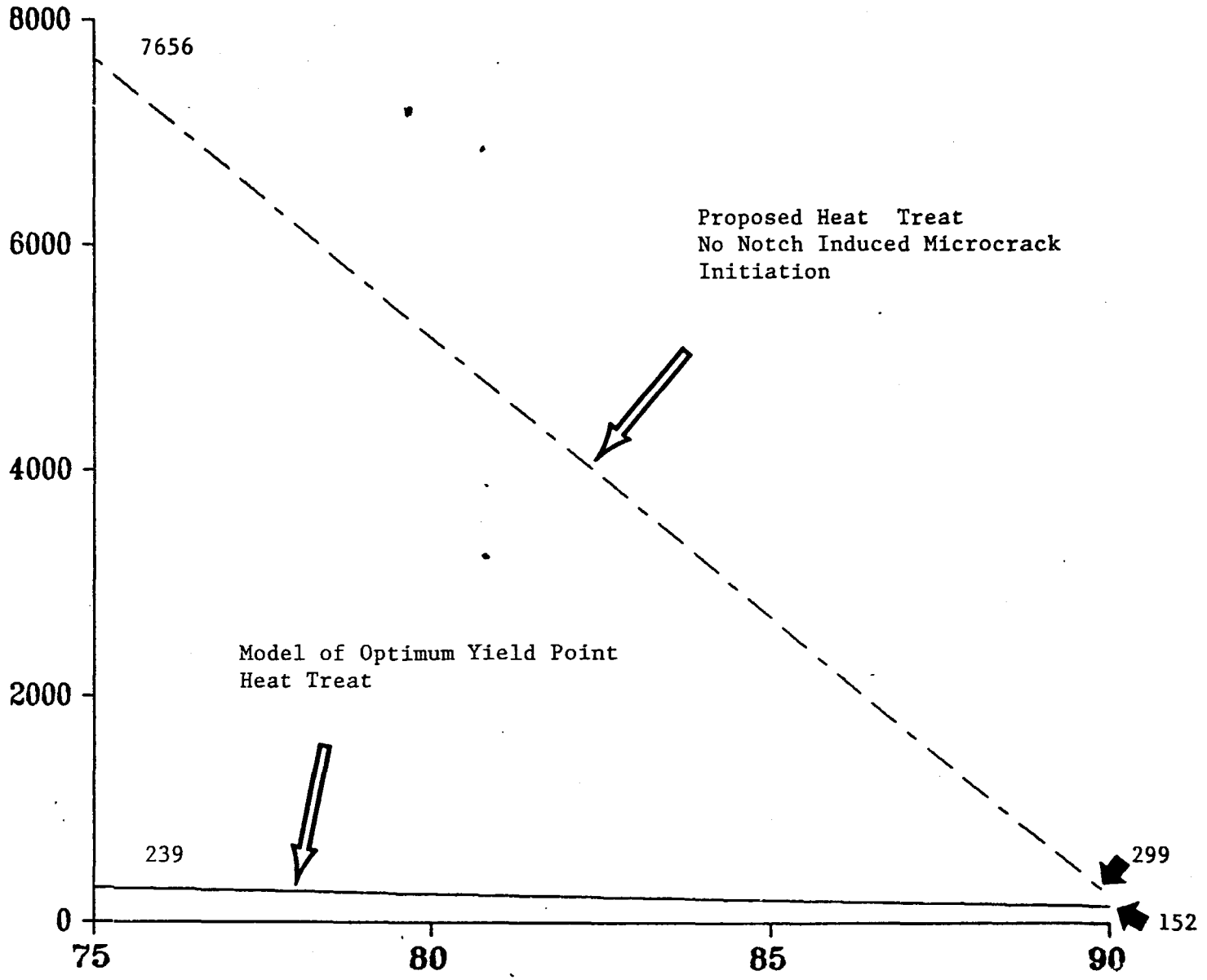

CLOSURE

Of all the calculations performed on test data from different solution and aging heat treatments, the underaged and critically aged specimens had their precipitates sheared by dislocations. This resulted in premature crack initiation at elevated temperatures, (where subsequent creep grain boundary movement occurred), as compared with unnotched specimens. Initiation was followed by crack propagation to premature ultimate fracture. In each case TEM analysis exhibited slipbands due to localized non-homogeneous deformation(8), where the dislocations sheared the γ' and γ' precipitates. (Figures 10, 13a, 14a).

In the proposed treatment, the specimens were overaged and the dislocations passed between their precipitated barriers (Figures 8, 11, 12). Premature crack initiation at elevated temperatures did not occur as compared with unnotched specimens, and this resulted in extended service life (Figure 15).

TEM micrographs confirmed in each case, that the dislocations bypassed the precipitates without shearing them(8) resulting in homogeneous high temperature deformation, in which Notch Induced Microcrack Initiation was eliminated. In every case the theory was in complete agreement with the experimental results of Reference 9.

The precipitate cracking characterized heretofore, when combined at identical locations with high temperature creep deformation, is the nucleation mechanism for premature crack initiation.

D. EFFECT OF SOLUTION TEMPERATURE

Decreasing the solution treatment temperature without changing the solution time, keeping the aging time and temperature constant, decreases the amount of alloying elements taken into the solution treated and quenched condition. This decreases the volume fraction of precipitates generated during aging, and decreases the precipitate size at the critical distance. However, the reduction in critical size does not effect the critical distance between spherical coherent precipitates and the maximum yield point associated with this distance.

Let's compare the behavior of Inconel 718, when the aging treatment is held fixed at 48 hours and 1350°F and the solution time held constant at 10 hours (Figures 11, 12). When the material is solution treated at 1950°F and creep rupture tested at 1000°F, Figure 11, the distance between precipitates is 39 Burgers vectors*. The specimen exhibits severe Notch Induced Microcrack Initiation at a shear yield point of 59 ksi(8). Reducing the solution temperature to 1800°F reduces the alloying elements available for precipitation and this decreases the critical particle size. Since the average distance between precipitates Ω, is closer now to the critical distance, than when solutioned at 1950°F, there will be a small increase in the particle size, resulting in an increase in the distance between precipitates from 39 to 41 Burgers vectors. Hence, there will be a

* A Burgers vector is the shortest atomic distance on a close packed glide plane.

corresponding increase in the yield strength to 61 ksi. Here, Ω is closer to Ω critical than at the higher solution temperature and Notch Induced Microcrack Initiation has been reduced but not eliminated. If the aging process is now applied with further reduction in solution temperature a critical dislocation line length is reached, together with its corresponding maximum yield point but with a smaller critical particle size.

Finally, by reducing the solution temperature to 1700°F the critical precipitate size is further reduced, and is surpassed by the aging treatment. Here the length of dislocation line segment goes beyond the critical length of 50 to 167 Burgers vectors with a corresponding reduction in yield strength from the critical value of 68 ksi to 58 ksi. This however satisfies the specification requirements set forth in AMS 5596 for plane stress deformation. The material is now overaged, and Orowans criteria(4), set forth in equation(8) is satisfied. The dislocation line segments now pass between precipitate particles without shearing them and Notch Induced Microcrack Initiation is completely eliminated.

Hence, reducing the solution treating temperature, decreases the amount of alloying elements taken into solid solution, which decreases the precipitate size at the critical distance. This does not alter the critical distance itself nor the maximum yield strength which occurs at the critical distance, when the dislocation line segment between spherical coherent precipitates, is bent to its maximum radius of curvature.

E. THE EFFECTIVENESS OF HARDNESS TESTING IN THE EVALUATION OF YIELD POINT STRENGTH.

The results of a plane stress static test at 1000°F on unnotched tensile specimens of Inconel 718*, show a tensile yield point of 135 ksi(8). This is in direct agreement with the yield point obtained by the alloy manufacturer, (International Nickel Co), when the material specifications(8) were established. Hence, the average length of dislocation line segment satisfies the critical dispersion size Ω_c, when the material shows the optimum yield strength at that temperature. However, the hardness tests on the specimens, showed a diamond pyramid hardness of 375, which was lower than the hardness of specimens from another procedure** that exhibited a lower yield point(8). The same lack of correlation occurred when identical specimen of the two heat treats were tensile tested at 1200°F by identical testing procedures(8). The answer lies in the change in microstructure that manifests itself in the high temperature behavior of the alloy between the onset of yield and the attainment of the ultimate strength. Thus, the failure of a room temperature hardness test to evaluate a high temperature condition is revealed.

* Solution treat for 1 hour at 1700°F ± 25°F followed by an aging treatment for 3 hours at 1325°F ± 15°F.

** The other procedure was to solution treat 1 hour at 1950°F ± 25°F followed by an aging treatment for 48 hours at 1350°F ±15°F, which showed a diamond pyramid hardness of 400 with a yield point of 129.5 ksi.

When the yielding of the gauge length is completed, many new dislocation sources are activated, with a resulting increase in the dislocation density. As the dislocation density increases, the moving dislocations are immobilized by interacting with newly formed stationary dislocations that pin them at their interior points. The barriers to dislocation motion are now so numerous that the dislocations remain pinned and the material is said to have work hardened. It is now impossible for further plastic deformation to occur, unless there is an incremental increase above the flow stress that will free a limited number of dislocations to produce an increment of strain. Consequently, the number of dislocations released in each incremental increase of stress are insufficient to cause an avalanche as happened previously at the yield point. The barriers to their motion will pin them after they move a short distance, and another increment of stress is required for plastic deformation to resume. During this process at 1000°F to 1200°F, there is an additional strain increment from grain boundary movement due to creep*.

The limit of the ratio of the amount of shear stress required to exceed the flow stress to free the dislocations from their barriers, to the amount of plastic strain increment caused by the resulting dislocation motion, as the strain increment approaches zero at that temperature, is called the elevated temperature work hardening coefficient. It is the physical quantity that signifies the conclusion of yielding, and the activation and retardation of plastic flow after yielding has ceased.

Hence, when the yield point is approached during a static tensile test at room or elevated temperature, two independent mechanisms dominate the plastic deformation at different times during the test:

a. The flow stress is the physical quantity that frees the immobilized dislocations from their precipitate barriers in avalanches, without an increase in the externally applied stress, and characterizes the shear yield point of the material.

b. The work hardening coefficient is the physical quantity that marks the conclusion of massive dislocation breakaway and characterizes the termination of yielding. It is the functional mechanism that dominates and controls the dislocation reactions, from the termination of plastic yielding up until the ultimate strength, at which time the specimen begins to neck down for ultimate fracture.

Consider now, the reduction in the yield point, when the critical dispersion size Ω_2 is surpassed, in overaged Inconel 718. Each dislocation line segment bows between widely spaced obstacles and passes between them. As the dispersion size increases, the process is characterized by Orowan's theory (Equation 6), and it requires a lower flow stress for each dislocation segment to surmount its precipitate barriers.

* If the tensile or creep test is allowed to continue over a sufficient time interval at an elevated temperature, the internal stress is further reduced by growth of precipitates, or recrystallization of strain free grains in the surrounding matrix which soften the material by reducing the intensity of the internal strains[4].

Upon increasing the applied stress to the ultimate stress, it is found that the ultimate stress also decreases with increasing aging time, and it is this stress that is estimated to a first approximation by a hardness test.

As the yield point is approached, the microstructure of the virgin material consists of undeformed grains, containing globular delta precipitates at the grain boundaries (Figure 3). The precipitates γ'/γ'' are the primary barriers that immobilize the dislocations to give the material its yield point strength*. A precipitation hardened alloy has its maximum yield point strength when the average dislocation line segment length is at the critical dispersion distance Ωc, and this is governed by the relation of Mott, Nebarro and Cottrell (Equation 5). When the alloy is overaged, Orowan's criteria (Equation 6) replaces that of Mott, Nebarro and Cottrell to relate the dispersion distance Ω with the flow stress[4]. The flow stress is the mechanism that controls precipitation hardening at the onset of the yield point where the alloy has the microstructure depicted in Figure 3.

During yield, there are an enormous number of dislocations that leave the material to give the alloy its plastic deformation, together with a severe increase in dislocation density, due to the activation of many dislocation sources. Each source will generate an almost unlimited number of dislocations, which are finally pinned by stationary dislocations and other barriers. These will then act as new barriers after yielding has terminated over the gauge length, due to the action of the work hardening coefficient. The work hardening coefficient is the physical quantity that controls the deformation, up until the ultimate strength where work hardening can no longer occur. The material has now deteriorated to a state of incipient ultimate fracture, and its microstructure has completely changed during the transformation that began with the onset of yield. The grains are now severely deformed due to work hardening and high temperature grain boundary creep movement. The precipitates are no longer useful as a strengthening mechanism after the material has seen extended service at 1200°F and above, where γ'/γ'' precipitates have enlarged with time, and γ'' has transformed into platelets of the delta phase.

* The precipitates γ'' and/or γ' are not seen at the magnification of Figure 3.

When the ultimate stress is reached, equations 5 and 6, the flow stress and the work hardening coefficient have no physical significance, and the results from hardness tests are inadequate to evaluate a heat treated item, for its yield strength or for its capacity to eliminate Notch Induced Microcrack Initiation*.

Hardness testing should be replaced by a static tensile or shear test at the service operation temperature, combined with a calculation of the average distance between precipitates. Analysis of the dispersion size, is to be done by the theory of Mott, Nebarro, and Cottrell when the critical distance exists between precipitates, (Equation 5), by and the criteria of Orowan, (Equation 6), when the critical distance between precipitates is surpassed by overaging the alloy.

* This was demonstrated by an example cited earlier in this section.

F. ELEVATED TEMPERATURE MECHANISM FOR YIELD STRENGTH REDUCTION

Evaluation of the mechanical properties of an alloy at elevated temperatures depends on a number of factors: (1) The implementation of the correct testing procedures, including the attainment of thermal equilibrium over the specimen in its furnace environment. (2) The stress distribution, i.e., whether plane stress or plane strain conditions prevail, and (3) The interpretation of time independent and time dependent mechanical properties as related to the material microstructure. Since in-service behavior for a specified time at a fixed operating temperature is equivalent to an extended aging operation at that temperature, it is sometimes convenient to demonstrate the structural changes that occur due to dislocation motion as a function of time, to explain the changes in the materials yield point. In this section, an analysis is made of the changes that manifest themselves in the microstructure and energy distribution of solution treated* and aged**. Inconel 718 specimens that were stress rupture tested below the yield stress, at elevated temperatures of 1100°F and 1400°F, respectively. From these experimental results, inferences are drawn that show the structural changes that act to reduce the yield point strength at elevated temperatures.

In the FCC lattice, exclusively on {111} planes and ⟨110⟩ directions, translational glide or slip is usually the principle mode of plastic deformation. However, rather than occurring by a continuous distribution of atomic sized shear displacements on planes a few atoms distances apart, the slip which accompanies large plastic strains takes place, with dislocations moving out of the material on relatively few planes thousands of atomic distances apart. Only the atomic bonds in the immediate vicinity of the slip plane undergo a change during the shift in position. The active slip planes are separated by large regions of undisturbed crystal which translate as blocks during localized deformation.

Unnotched specimens were tested at 1100°F at a constant applied stress of 120 ksi***, and the results were examined by TEM analysis(8). {111} planar slip bands appeared on the external surfaces, signifying that the dislocations moved exclusively by slip on {111} planes, as they cut through the coherent γ'/γ'' precipitates, and were annihilated at the external surface. (Figure 13a). This localized deformation mechanism (slip bands separated by large regions of undisturbed crystals), occurred whenever the specimens were tested at temperatures low enough for little or no growth of the γ'/γ'' particles. Ultimate fracture was by stress rupture after 1.4 hours.

* Solution treated for 1 hour at 1950°F ± 25°F.

** Aged for 48 hours at 1350°F ± 15°F.

*** The static yield point stress at this temperature is 130 ksi(8).

Identical specimens were tested at 1400°F at 30 ksi, and structural changes were observed as compared to the results of the 1100°F tests. δ needles precipitated within the grains depleting the γ' strengthening capability. At 1400°F the γ' particles grew to 750Å diameter, and γ' to plates 500Å thick and 4000Å long, and both precipitates were still coherent with the matrix(8). Slip bands were not observed but dislocations were seen 'entangled with γ' and in some cases as loops around γ' particles', and the deformation was homogeneous(8), (Figure 13b). The results are consistent with the bypass mechanism of Orowan's criteria (Equation 6), where particle growth during the test placed the specimen in an overaged condition that exceeded the critical distance Ω_c, a condition that would reduce the critically resolved shear stress. The specimen failed after 385 hours as compared to 1.4 hours at 1100°F. This suggests a possibility of δ phase stress raisers combined with creep for crack initiation at the lower temperatures.

The above results are analogous to the conclusions drawn from an investigation of Waspaloy at 1000° --> 1400°F. Here, the dislocations sheared γ' particles whose average distance was less than Ω_c and circumvented γ' particles with $\Omega > \Omega_c$ (11).

Hence it is demonstrated that, as Ω_c is exceeded by the growth of precipitates during high temperature operation, the dislocations pass between their obstacles, and the critical resolved shear stress is reduced by the same mechanism that eliminates Notch Induced Microcrack Initiation.

There are other phenomena acting under the effect of high temperature microstructural changes that lower the critical resolved shear stress: (1) There is the transformation of entire γ' particles to δ phase platelets, which depletes the material of its strengthening capability by removing the precipitate barriers, (2) The process of cross slip occurs primarily in a two phase alloy, when the particle spacing Ω is at least ten times the particle diameter(2) and the energy reduction of the system is favorable(2). Cross slip occurs because a perfect Burgers vector in an FCC lattice a/2 <110>* always lies on the line of intersection of two intersecting {111} planes, so that a perfect dislocation with screw orientation can easily change its slip plane**. Then there are the thermally activated processes that include: (3) Thermal glide, (4) Climb and (5) Jog dragging.

* a is the lattice parameter of the crystal.

** Cross slip is actually considered a special case of the bowing out mechanism of the Orowan criteria, which gives the dislocation line an extra degree of freedom compared to the Orowan mechanism where the dislocation stays in one plane. See the discussion (Reference 6).

Let a dislocation line segment be pinned by coherent precipitates at an elevated temperature*, (Figure 16), and let a stress σ_o be required to overcome this barrier. Here σ_o is the stress required to bend the dislocation line segment to its limiting radius of curvature when $\Omega = \Omega_c$. Depending on the elevated temperature, it is possible that lattice vibrations may cause thermal energy fluctuations that will increase the applied stress so that the required external force exerted on the stress field of the precipitates may be less than σ_o and the barrier may be overcome by the applied stress σ.

* This model was originally proposed by Cottrell to analyze the breaking away of a dislocation line segment from an atmosphere of carbon impurity atoms in steel. However, similar arguments apply to other systems since the interaction energy is of a similar form[8],[12].

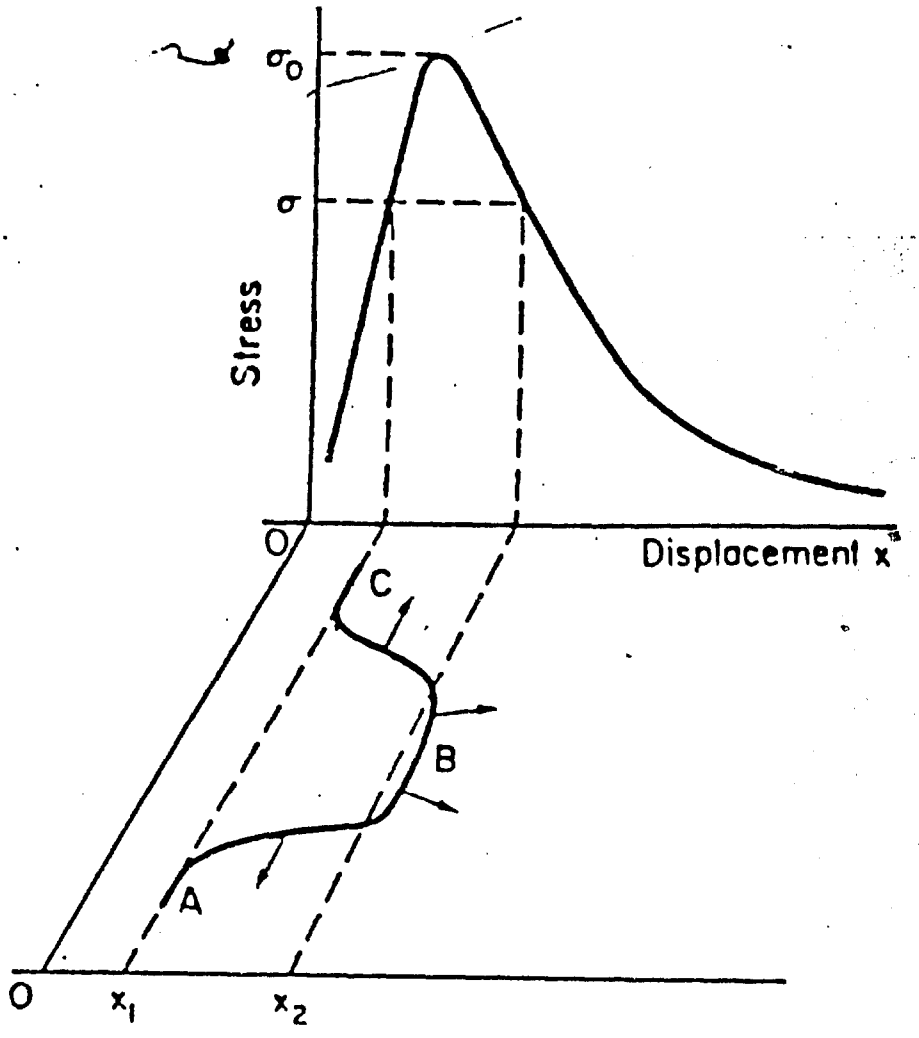

Figure 16: Stress vs displacement for a dislocation line segment, as it overcomes its barrier at elevated temperatures, with the aid of a thermal stress fluctuation. (From A.H. Cottrell (1957) Properties of Materials at High Rates of Strain, Inst Mech Eng, London)

The thermal energy supplied by the lattice vibrations is sufficient to bend the dislocation line segment ABC to its limiting radius of curvature, in order to pass the saddle point σ_o, and surmount the potential energy barrier. This extra energy supply increases with increasing temperature to cause the critical resolved shear stress to decrease as a function of temperature. The above process is sometimes called thermal glide, since it requires the imparting of thermal energy to initiate slip, at the applied stress σ. The rate of break-away of dislocation loops per unit time, is given by Cottrel(12) to be proportional to: (a) The number of pairs of precipitates separated by Ω_c, (b) The vibrational frequency of the lattice and (c) e x p(-E/KT) where E is the thermal energy supplied to bend the dislocation segment to its limiting radius of curvature, T is the absolute temperature, and K the Boltzmann constant. Cottrell and Bilby(13) also proposed that once the barrier is surmounted, the loop will expand under the applied stress and pull the remainder of the dislocation from the anchorage by an unzipping process(8). Hence, once the segment has surmounted its barrier, the entire dislocation is free to move.

A dislocation may move by slip or conservative motion which occurs on a slip plane* and in a slip direction. It may also move by climb or nonconservative motion, where the dislocation moves out of its glide surface by the diffusion of vacancies to or from it, depending on which direction the dislocation climbs.

Some of the vacancies are present before deformation occurs and others are generated during the deformation process. Consider the oversimplified case of an edge dislocation line in a crystal surrounded by a number of vacancies (Figure 17a). The vertical row of atoms above the core is in compression, and the space below is in tension. The original position of the vacancy is designated by a +, and the sequence of atoms as they move into the vacancy numbered 1-8 are shown in black (Figure 17b). Vacancies are not stationary in the crystal lattice and if the temperature is raised, thermal energy is supplied, which the lattice vibrations impart to one of the neighboring atoms so that it moves into the hole. Thus, the vacancy has moved from its original position to the lattice site vacated by atom 1. (Figure 17c). In doing so the compressive stress above the core has been reduced, lowering the energy of the alloy. This reduction in system energy continues, (Figure 17c shows the sequence), as the vacancy moves toward the dislocation core where the maximum energy reduction occurs in position 8 of Figure 17b. The vacancy movement into the dislocation core allows the dislocation to move up one atomic position in the plane of the cross section. (Figure 17c). If an entire row of vacancies moved into the core in a line extending into the paper, the edge dislocation would move up one atomic position, because an entire row of atoms was removed. Similarly, if a row of atoms is introduced in the space just below the extra half plane, the dislocation line moves down one atom spacing in the opposite or negative direction.

* The plane is defined by the dislocation line and the Burgers vector.

The additional row of atoms necessary for downward motion would be obtained from the neighboring atoms in the immediate vicinity of the dislocation line, so that many vacant lattice sites would be created. Motion upward would, in a similar manner, require the dispersion of extra atoms into the crystal lattice. In either case, the motion of an edge dislocation normal to its slip plane, is governed by the rate of diffusion of atoms away or toward the edge of the extra half plane. Such a dislocation motion is called climb and occurs at a much slower rate than glide, unless the edge segment is very small or the temperature is very high. Because vacancies are either created or annihilated during climb, the total volume of the crystal is not conserved, and this type of motion is called nonconservative.

Slip in an ordinary crystal is not confined to a single plane but, as described earlier, to a family of crystallographically equivalent planes and a family of crystallographic equivalent directions. Under these circumstances it is very probable that two moving dislocations intersect and produce a unit step in each other. This unit step is called a jog. After intersection, continued motion of one of the dislocations can occur only if the jogged segment moves by climb while the other two segments on parallel planes remain in their slip system and move conservatively. Here, the resistance to glide motion does not come from the interaction of the moving dislocation with other obstacles but from the retardation of the jog produced by the intersection. This type of motion is called 'jog dragging'.

Now consider a case where the critical distance between precipitates Ω_c is exceeded so that $\Omega > \Omega_c$. The dislocation line segment has exceeded its limiting radius of curvature, and passes between precipitates in accordance with Orowans criteria, leaving dislocation rings around each precipitate (Figure 8). At temperatures exceeding 1/2 the melting temperature in coarse grained alloys with large applied loads[7], the Orowan rings will climb out of their slip plane, and provide the rate determining process for deformation[7].

Although the models presented above are oversimplified, they represent the mechanisms that contribute to high temperature deformation of the alloy*, (at $T \geq 1/2\ T_m$**), by nonconservative dislocation motion within the grains. This leads to a very important result:

* Inconel 718 falls into this category in the range 1000 - 1400°F.

** T_m is the temperature of solidification.

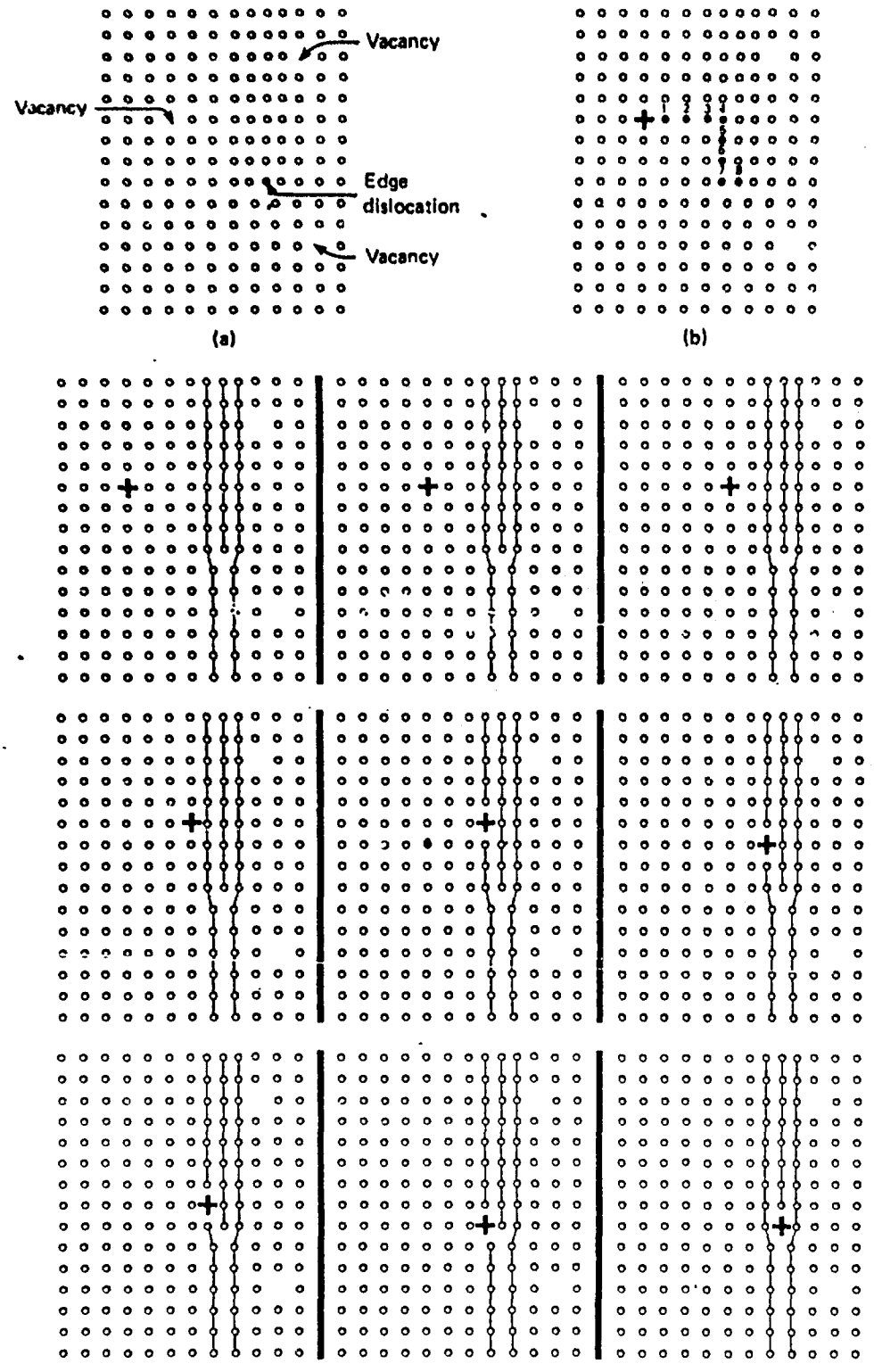

Figure 17 - Schematic illustration of the movement of a vacancy to the core of a dislocation, causing the dislocation to climb by one atom position. (Taken from C.K. Brooks, Heat treatment, structure and properties of nonferrous alloys American Society for Metals (1982))

The above high temperature deformation by nonconservative dislocation motion, combined with coherent precipitate shearing at the same location within a grain, serves as a mechanism for intragranular crack initiation, at stress concentrations such as δ phase platelets or manufacturing defects. Although this result does not explain the predominately intergranular nature of the crack propagation (presented in Section A), it allows for the possibility of intragranular crack initiation, followed by grain boundary (intergranular) propagation.

In this section it was shown, that microstructural changes occur during service that change the material properties of the alloy at specified elevated temperatures. These property changes include: (a) Growth of precipitates, (b) Allotropic transformation of $\gamma' \rightarrow \delta$, (c) Thermal glide, (d) Dislocation climb, (e) Jog dragging, (f) Grain boundary deformation. These property changes may either produce or eliminate the conditions for Notch Induced Microcrack Initiation, and are the factors that determine the time-temperature limits of material serviceability.

G. THE TRANSFORMATION OF GAMMA DOUBLE PRIME TO DELTA

The allotropic change in the solid state:

γ'' (Ni_3Cb) ----------> δ (Ni_3Cb) (1)
Body centered . Orthorhombic
Tetragonal

occurs in three structural forms:

1 - Platelets
2 - Cellular
3 - Globular

"There have been no reports of cellular δ in any commercial γ'' strengthened alloy[14][15]." Analysis of the transformation to globular δ at the grain boundaries of Inconel 718 depletes the yield strength of this alloy, however, the reaction inhibits long range grain boundary sliding and is therefore, advantageous. The cellular and globular forms of orthorhombic Ni_3Cb will not be covered, but a model is presented to analyze the formation of platelets, since the platelets form a geometric configuration that is detrimental to the serviceability of the material.

There are imperfections that exist in a crystalline solid, which impart properties to the material to determine its usefulness for industrial applications. These are: (1) point, (2) line and (3) surface defects. A vacancy is an example of a point defect, a dislocation is a line defect, and a stacking fault is what is known as a surface defect. It is the latter defect that provides the condition for nucleating the γ'' -> δ transformation.

A new phase may nucleate in a solid by: (1) A number of atoms find themselves in a statistically favored equilibrium position to form a structure that lowers the energy of the system at that temperature. One example of this is the formation of ferrite from austenite iron as the temperature is lowered quasi-statically from the austenite region to the transformation temperature. Once a unit cell is formed, it will grow as a nucleus, and (2) A mechanical change may occur in a solid where the material is displaced from its ordered state. One example is the formation of a dislocation by a cutting displacement and rebonding process within the metal, or by the operation of a Frank-Read source. Another example of a mechanical displacement is the dissociation of a perfect dislocation into two partials separated by a region of stacking fault. Upon separation of a perfect dislocation into two partial dislocations of like signs, the partials exert repulsive forces on one another, and the total elastic energy of a body containing two parallel partial dislocations is reduced by their separation. However, as the partials separate, the width of the ribbon of stacking fault is increased with an associated increase in energy. The resulting equilibrium distance between two partials is determined by the conditions that the attractive force due to the increase in stacking fault energy balances the mutual repulsion of the partials. After dissociation, the energy of the extended dislocation, including the newly formed stacking fault, is less than the energy of the perfect dislocation. It is this separation of partials, which occurs as a perfect dislocation dissociates, inside the body centered tetragonal γ'' precipitate particle, which may be the nucleation site for the orthorhombic δ phase.

Some of the most often made statements about Inconel 718 address themselves to high temperature crack initiation and the γ' ---> δ phase transformation: 'At present no single mechanism or combination of mechanisms have been put forth which explains how these metallurgical variables interact to control a metal's microfissuring susceptibility[17]' and, 'Is there any crystallographic relationship between the γ' and δ phases which affects the δ transformation[18].' Each of the above authors were searching for a mechanism or physical relationship that provides an in-depth solution to both problems. The first of these has already been analyzed earlier. An atomic model will now be presented that postulates the nucleation of δ phase platelets within the γ' structure, and its subsequent depletion of γ' precipitates. The two phenomena will then be combined by introducing the proposed heat treat procedure, which completely eliminates Notch Induced Microcrack Initiation and considerably reduces the Widmanstätten needles of the δ phase (platelets).

Figure (18) shows a TEM micrograph of a thin film, where an intragranular δ needle has grown through three separate γ' plates[18]. The δ phase precipitates as needles or lathes along (111) family planes of the face centered cubic γ matrix. This indicates that the δ needles either nucleated at or grow preferentially through γ' plates[18].

The nucleation of the δ needles appear to be connected with the occurrence of stacking faults which are frequently observed within γ' plates[14]. The body centered tetragonal γ' structure is made up of close packed ordered planes, stacked in a six layer sequence, A B C D E F A B C D E F. However, as a dislocation dissociates, the displacement due to the dissociation may produce a stacking fault, with the same nearest neighbor atom relationship as the above γ' structure, but with the stacking sequence altered from A B C D E F A B C D E F to A B C D E F A B A B C D E F. The four layers of atoms having A B A B stacking, make up the structure of the orthorhombic δ phase. In other words, the γ' faults have the same structure as the δ needles[18] and the authors suggest[18] that δ nucleation occurs by the growth of these faults into the matrix forming needles which replace the γ' plates, and produce a γ' - free zone around the δ needles. This depletes the alloy of the major hardening phase in Inconel 718[13, 18].

Figures (19) and (20) are optical micrographs taken from the CBF segments that were given the proposed heat treatment. Note that the majority of the δ phase exists as grain boundary globular δ, while most of the Widmanstätten needle structure has been eliminated. This is because this solution treatment is applied for 10 hours at 1700°F and is sufficient to dissolve the detrimental δ platelets that transformed from γ' during high temperature service. The existing GE procedure B50T69B*, calls for 1 hour solution time at 1700°F which is inadequate for diffusion of the platelets into solution.

* See Figure 2 for General Electric procedure.

Figure 18 - TEM micrograph of a thin film of a Ni - Fe - Cr - Cb alloy showing a thin δ needle normal to the foil surface, growing through three γ' plates. The lattice parameters of the δ phase was determined by electron diffraction to be: a ≃ 5.11Å, b ~ 4.25Å, c ~ 4.56Å (Taken from Reference 16).

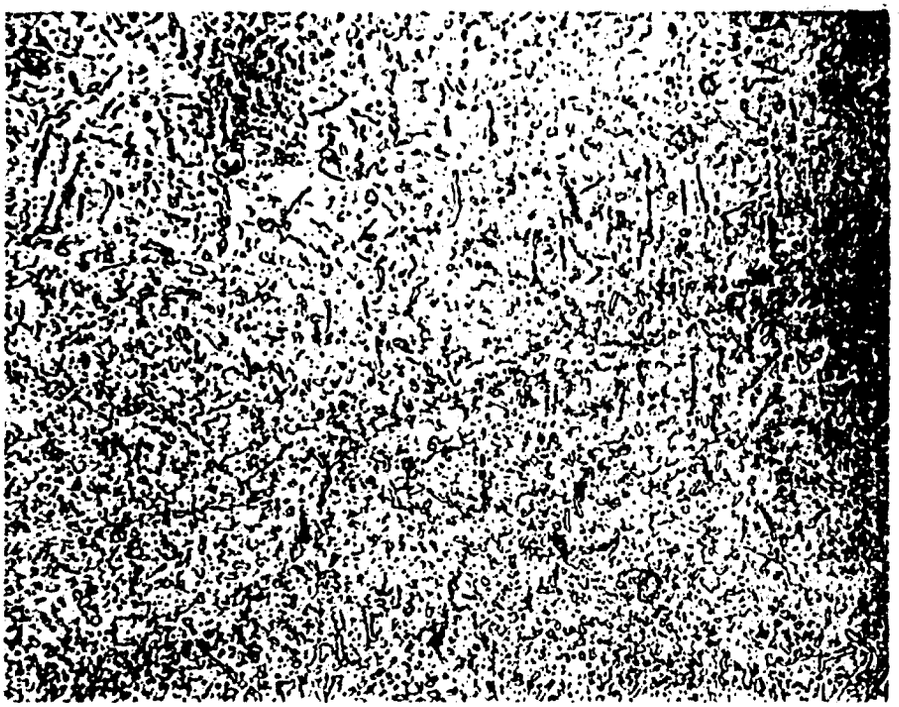

Figure 19 - 1000x (Marbles etch) Optical micrograph of the microstructure of Inconel 718 taken from a Compressor Rear Frame removed from service and given the proposed heat treat. The majority of the needles have been eliminated. Compare with the Widmanstatten needle structure of Figure 2.

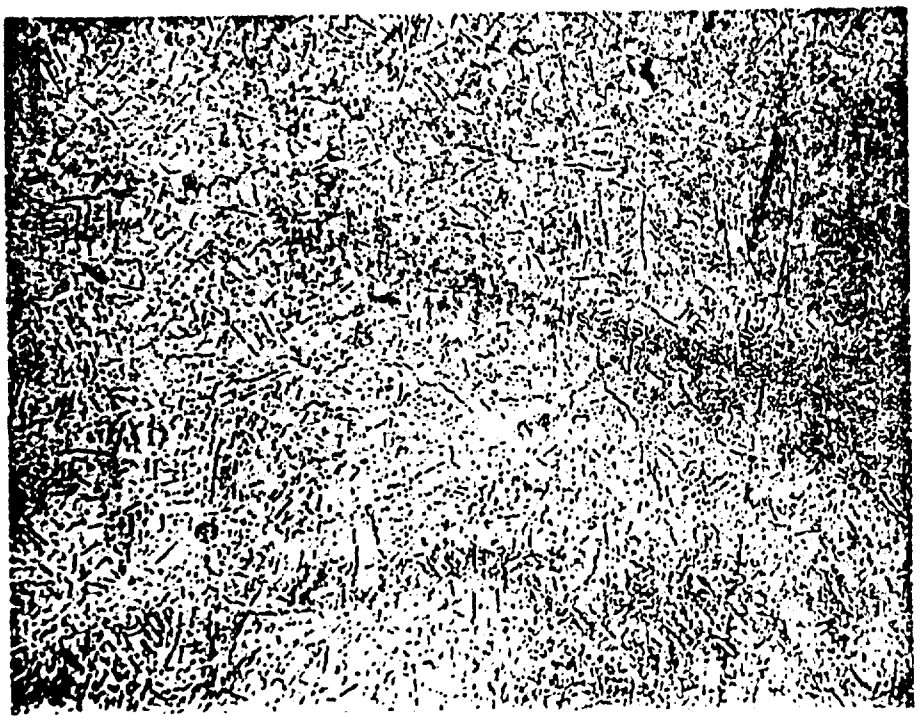

Figure 20 - 500x (Marbles etch) Same as Figure 19, except at lower magnification.

H. CLOSURE

This work has demonstrated the practical applications of dislocation theory, which quantitatively relates atomic parameters to macroscopically measured quantities, to evaluate atomic level microstructural changes that eliminate Notch Induced Microcrack Initiation.

The concept of a dislocation was first introduced into elastic theory, in the early 1900's by Volterra and by Timpe(19). In the early 1930's it was observed experimentally that metallic crystals deformed at an order of magnitude of 10 below the theoretically predicted strength. This phenomena stimulated sufficient interest and concern in 1934, that three scientists: G.I. Taylor, M. Polanyi and E. Orowan, working independently of each other, postulated the existence of a line defect within the crystal lattice, whose motion at low stress levels, permitted slip, the mechanism of plastic deformation to occur(19). This defect is called a dislocation. As the dislocation line moved through the crystal, bond breakage across the crystal occurred consecutively, (as the line overcame the Peierls stress at each atomic location), rather than simultaneously, as must be the case in a perfect lattice(20). The dislocation concept was developed by Burgers, Mott, Nebarro, Cottrell, Bilby and Stroh (1939-1952), at a time when no one had ever seen a dislocation, and it was considered by most as a figment of the imagination, that successfully explained most phenomena of mechanical properties, without having the capacity to quantitatively predict these properties. The problem lay in the fact that it was a very formidable task to relate quantities such as Burgers vector, lattice parameters, stacking fault energy, and atomic distance between precipitates, to macroscopically measured quantities of practical significance.

Dislocations were first seen in the early fifties, by Hedges and Mitchell in silver halide crystals, followed by transmission electron microscopy in 1956 by Hirsh, Horne, and Whelan and independently by Bollman(19).

The first meaningful practical application occurred in 1962 when D. Kuhlmann - Wilsdorf derived an expression that predicted the work hardening coefficient for Stage II plastic deformation, in terms of basic atomic parameters for pure F.C.C. metals(21). She clarified some basic principles and showed that the work hardening coefficient was insensitive to many changes in detailed dislocation behavior(21). Bilby, Cottrell and Swinden(22) derived an expression for a continuous distribution of dislocation as a function of the shear crack displacement for an infinite(22) and finite(23) plate. Here the relative displacement Ø(c) divided by the Burgers vector b, gave the number of dislocations within the plastic zone that broke away from their barriers to produce the displacement Ø(c). Their results were quantitatively related to acoustic emission counts, with Burgers vector b and dispersion size Ω, to solve for crack length(3), and thus develop a quantitative nondestructive testing method.

The present work presented heretofore has been one of the first applications, where dislocation theory was used to directly solve a reliability problem in production. The dynamic reactions that occurred at the atomic level, as the parameters of dispersion size Ω, Burgers vector b, particle diameter d, related the theory of the flexibility of the dislocation line segment with the effect of the flow stress, to determine if the dislocation will cut or pass between precipitates, in order to eliminate Notch Induced Microcrack Initiation, and intimately effect the serviceability of the final part.

I. CONCLUSIONS

1. Notch Induced Microcrack Initiation is a primary cause of premature high temperature crack initiation, occurring in Inconel 718 alloy. This shortens the service life of engine components such as the TF39 compressor rear frame and the F100 Augmentor shoulder pin. Laboratory tests on the proposed heat treatment have proven to completely eliminate Notch Induced Microcrack Initiation from this alloy. This resulted in an increase of the service life, and in an improved material.

2. The in-service transformation from gamma double prime to delta platelets in Inconel 718 lowers the yield point strength by depleting the precipitate and produces stress concentrations within the grains to adversely effect the ductility and fracture characteristics of the alloy. A microstructural analysis of a compressor rear frame heat treated by the proposed procedure, shows a substantial reduction of the delta phase, as compared to the microstructure shortly after removal from service, while the tensile strength of the heat treated item remained within specification limits.

3. Notch Induced Microcrack Initiation is due to the way dislocations break from their precipitate barriers in reference to a average critical distance between the precipitates. When the average distance between precipitates is less than or equal to the critical distance, the dislocations will shear through the coherent particle, creating localized plastic deformation. When this is combined at identical locations with high temperature creep deformation a crack will nucleate prematurely.

4. When the average distance between precipitates is greater than the critical distance, the dislocations will pass between the precipitates without cracking them and Notch Induced Microcrack Initiation does not occur.

5. Decreasing the amount of precipitate in solid solution lowers the precipitate size at the critical distance, but does not alter the critical distance itself, or its maximum yield point. It is this critical distance that must be exceeded in overaging spherical coherent precipitates, in order that the dislocations pass between them.

6. The results of hardness testing are inadequate to accurately evaluate the heat treatment of a precipitation hardened industrial alloy. Hardness testing should be replaced by a static tensile or shear yield point test at the service operating temperatures, combined with a calculation of the number of atomic distances between precipitates.

7. For a material that operates at elevated temperatures, the reduction in the maximum yield point strength with increasing temperature, in a precipitation hardened alloy, is due to a reduced critical resolved shear stress, which is caused by:

a. The critical distance between precipitates being exceeded by growth of the particles at the operating temperature.

b. The γ' --> δ transformation removing the strengthening mechanism.

c. Thermal fluctuations that provide additional energy to reduce the shear stress required for the dislocations to break from their barriers, and for diffusion of vacancies to permit within grain deformation due to nonconservative dislocation motion.

d. Grain boundary deformation due to creep.

8. Microstructural changes occur during service that change the material properties of Inconel 718 at elevated temperatures. These property changes may either produce or eliminate the conditions for Notch Induced Microcrack Initiation, and are the factors that determine the time-temperature limits of material serviceability.

J. REFERENCES

1. D. J. WILSON
Sensitivity of the Creep-Rupture properties of Waspaloy sheet to Sharp-Edged Notches in the Temperature Range of 1000°F-1400°F. Journal of Basic Engineering, Trans ASME, Vol 94, No 1, Series D; P 13-21 (1972).

2. G. S. ANSELL
'Mechanical Properties of Two-Phase Alloys,' Physical Metallurgy, ED. R. W. Cahn, Second Edition, P 1083, North Holland Pub Co (1974)

3. H. A. FELDSTEIN
A Mathematical Analysis Which Relates Acoustic Emission Counts from a Dislocation Source to Crack Size II. Proc: 16th Symposium on Nondestructive Evaluation, San Antonio Texas, Marriott Riverwalk Hotel, (April 21-23 1987)

4. A. H. COTTRELL
Dislocations and Plastic Flow in Crystals, P 127-129, Oxford University Press, Amen House E. C. 4 (1965).

5. D. HULL
Introduction to Dislocations, P 80, Pergamon Press (1969)

6. A. KELLY
'Theories of Precipitation and Dispersion Hardening' in: Electron Microscopy and Strength of Crystals, P 947-971, John Wiley and Sons, (1963)

7. H. GLEITER and E. HORNBOGEN
Precipitation Hardening by Coherent Particles, Material Science and Engineering, Vol 2, P 285-302, Elsivier Publishing Co., (1967/1968)

8. INCO ALLOYS INTERNATIONAL
Int. Nickel Co., Huntington Alloy Div, 4717752, Specifications for Inconel Alloy 718.

9. D. J. WILSON
Relationship of Mechanical Characteristics and Microstructural Features to the Time-Dependent Edge-Notch Sensitivity of Inconel 718 Sheet, Trans. ASME Journal of Engineering Materials and Technology, P 112-123 (April 1973)

10. R. COZAR and A. PINEAU
Morphology of γ' and γ'' Precipitates and Thermal Stability of Inconel 718 Type Alloys, Metallurgical Transactions, Vol 4, P 47-59, (January 1973)

11. D. J. WILSON
The Dependence of the Notch Sensitivity of Waspaloy at 1000°F-1400°F on the Gamma Prime Phase, Journal of Basic Engineering, Trans ASME (in print at time of Publication).

12. A. H. COTTRELL
'Deformation of Solids at High Rate of Strain', The Properties of Materials at High Rates of Strain, Inst Mech Eng, London (1957)

13. A. H. COTTREL and B. A. BILBY
Proc Phys Soc A, Vol 62, P 49 (1949)

14. I. KIRMAN
Precipitation in the Fe-Ni-Cr-Nb System, Journal of the Iron and Steel Institute, P 1612, (Dec 1969)

15. C. T. SIMS and W. C. HAGEL ED
The Superalloys, Chap 4, P 113, Chap 7, P 197, John Wiley and Sons, New York (1972)

16. I. KIRMAN and D. H. WARRINGTON
The Precipitation of Ni_3Nb Phases in a Ni-Fe-Cr-Nb Alloy, Metallurgical Transactions, Vol 1, P 2667, (October 1970)

17. R. G. THOMPSON, J. R. DOBBS and D. E. MAYO
The Effect of Heat Treatment on Microfissuring in Alloy 718, Welding Research Supplement, Welding Journal, Vol 65, No 11, P 299-S (Nov 1986)

18. J. P. COLLIER, S. H. WONG, J. C. PHILLIPS, and J. K. TIEN
The Effect of Varying Al, Ti, and Nb Content on the Phase Stability of Inconel 718, Metallurgical Transactions A, Vol 19A, P 1657 (July 1988)

19. J. WEERTMAN and J. R. WEERTMAN
Elementary Dislocation Theory, P 3-4, The Macmillan Company, New York (1964)

20. R. W. HERTZBERG
Deformation and Fracture Mechanics of Engineering Materials, P 42, John Wiley and Sons, New York, (1976)

21. D. KUHLMANN-WILSDORF
A new theory of Work Hardening, Transactions of the Metallurgical Society of AIME, Vol 224, P 1047, (October 1962)

22. B. A. BILBY, A. H. COTTRELL, and K. H. SWINDEN
The Spread of Plastic Yield from a Notch, Proc Royal Society, Vol A 272, P 304, (1963)

23. B. A. BILBY, A. H. COTTRELL, E. SMITH, and K. H. SWINDEN
Plastic Yielding from Sharp Notches, Proceedings of the Royal Society, Vol A 279, P 1 (1964)